The Science And Engineering of Durable Ultralow PGM Catalysts

Fernando Garzon

Los Alamos National Laboratory

May 15th 2012

FC010

This presentation does not contain any proprietary, confidential, or otherwise restricted information

Los Alamos NATIONAL LABORATORY EST. 1943 · BALLARD power to change the world · THE UNIVERSITY of NEW MEXICO · UNIVERSITY of DELAWARE · OAK RIDGE National Laboratory

Overview

Timeline

- Project start date:03/2010
- Project end date:03/2014
- Percent complete: *60%*

Precious metal loading:	~0.2 mg/cm^2 (2015 target)
Cost:	< 3$/kW (2015 target)
Activity (precious-metal based catalyst):	0.44 A/mgPt @ 0.90 V
Surface area activity:	720 µA/cm^2 @ 0.90 V
Electrocatalysis support loss:	<30 mV after 100 hrs @1.2V
Electrochemical surface area (ESA) loss:	<40% (after cycling protocol)

Barriers

- COST: High performance catalysts enabling ultralow precious metal loadings are required to reduce cost
- PERFORMANCE: Voltage losses at the cathode are too high to meet efficiency targets. Loss of electrochemical surface area can occur as a result of catalyst migration and agglomeration

Budget

- Total project funding
- DOE share: $6M
- Contractor share: $529K
- Funding for FY11: $280K
- Proposed funding for FY12: $1.1M

Partners

- Ballard Fuel Cells, UNM, UD
- LANL

Los Alamos NATIONAL LABORATORY EST. 1943 | BALLARD power to change the world | THE UNIVERSITY of NEW MEXICO | UNIVERSITY of DELAWARE | OAK RIDGE National Laboratory

Collaborations and Task Assignments

- Theoretical Understanding Of Roles Of PGM Catalyst Shape, Size, Support Interactions And Catalyst Layer Architecture On Cathode Mass Activity And Durability
  - Optimization Of PGM Catalyst Morphology With Guidance From Computational Studies (LANL)
  - Optimization Of Catalyst Layer Architecture With Guidance From Microstructural Simulations (Ballard)
  - Understanding catalyst Particle nucleation and growth (UNM)
- Experimental Synthesis And Characterization Of New Geometry PGM Catalysts
  - Synthesis of Novel Pt Nanoparticles (UCR, UNM, LANL)
  - Synthesis of Pt Nanowires (UCR, UNM, LANL)
- PGM Structural Characterization by TEM, XRD, Neutron Scattering
  - HRTEM Morphology Studies (ORNL) (UNM)
  - Advanced X-ray Diffraction Studies (LANL)
  - Neutron Scattering Studies (LANL)
  - Thermal and Thermodynamic Characterization of PGM catalysts (UNM, LANL)
  - Electrochemical Characterization of PGM catalysts (LANL, UCR)
- Understanding Catalyst Nucleation And Support Interactions
  - Studies Of Precursor-Support Interactions (UNM, LANL)
  - PGM-Support Interaction Studies (UNM)
- Fuel Cell Testing Of Novel PGM Catalysts (LANL, Ballard)
  - Testing of novel catalysts in fuel cells (LANL, Ballard)
  - Fuel cell post testing materials characterization (LANL, ORNL)

- *LANL*
  - *Fernando Garzon*
  - *JoseMari Saniñena*
  - *Mahlon Wilson*
  - *Neil Henson*
  - *Ivana Matanovic*
- *UNM*
  - *Prof. Abhaya Datye*
  - *Elena Berliba-Vera*
  - *Andrew DelaRiva*
  - *S. Michael Stewart*
- *ORNL*
  - *Karren More*
  - *Kelly Perry*
- *BALLARD*
  - *Siyu Ye*
  - *David Harvey*
- *UD*
  - *Prof. Yushan Yan*
  - *Shaun Alia*
  - *Yanqi Zhang,*
  - *Zhongbin Zhuang*

Project Objectives – Relevance

•Development of durable, high mass activity Platinum Group Metal cathode catalysts - enabling lower cost fuel cells-*Synthesis and characterization of three new families of Low PGM catalysts LANL UD ORNL*

•Elucidation of the fundamental relationships between PGM catalyst shape, particle size and activity-will help design better catalysts-*DFT models for novel Pt nanotubes LANL, Pt nucleation and dispersion on carbons UNM*

•Optimization of the cathode electrode layer to maximize the performance of PGM catalysts-improving fuel cell performance and lowering cost-*Advanced microstructural catalyst layer model development Ballard*

•Understanding the performance degradation mechanisms of high mass activity cathode catalysts – provide insights to better catalyst design. *DFT models for particle reactivity, Free Radical scavenging MEAs LANL; Nanoparticle growth model and experimental validation UNM*

•Development and testing of fuel cells using ultra-low loading, high activity PGM catalysts-Validation of advanced concepts *LANL &Ballard*

•IMPACT: This project will help lower the cost and the precious metal loading of PEM fuel cells and improve catalyst durability

Approach

- Use contemporary theoretical modeling and advanced computational methods to understand and engineer the new catalysts and catalyst layers
- Model and design appropriate catalyst architectures to maximize the performance of our novel catalysts
- Investigate catalyst-support interactions and their effects on durability and mass activity
- Study and test the performance of the catalysts in electrochemical cells, single cell-fuel cells and fuel cell stacks
- Extensively characterize new materials before and after fuel cell operation

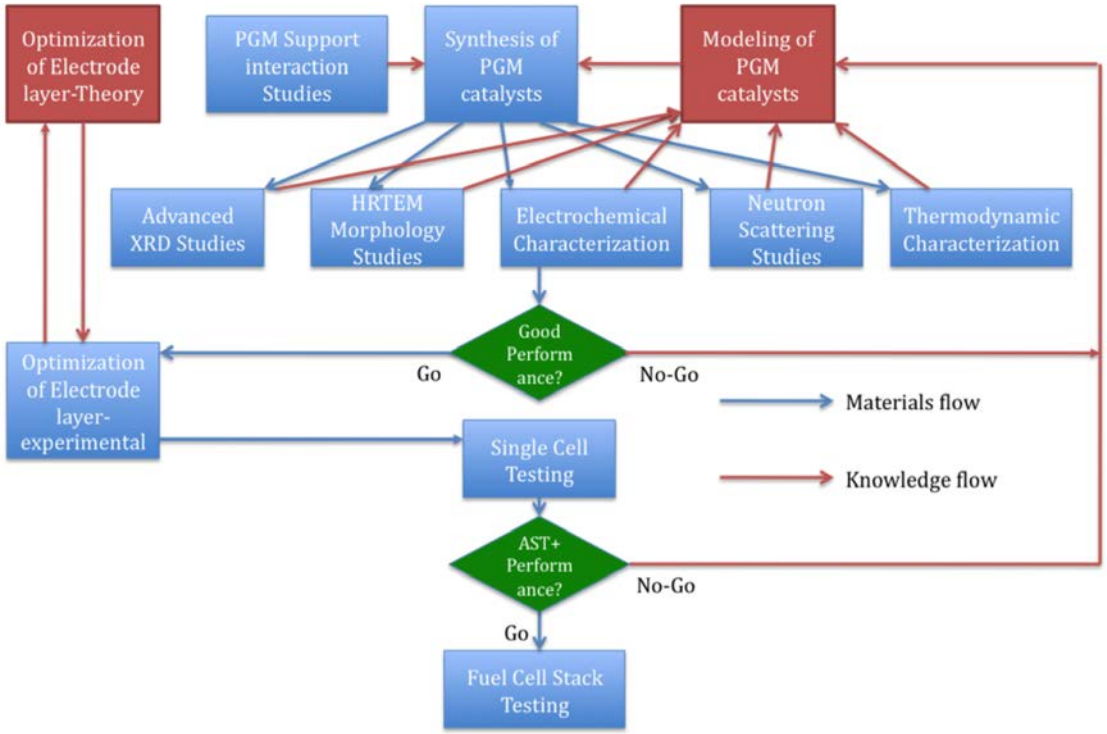

DFT and MD Modeling Novel Pt Catalysts

Reducing the ORR overpotential / cost:

(1) alloying platinum with platinum group metals

(2) nanostructures: nanotubes and nanoparticles

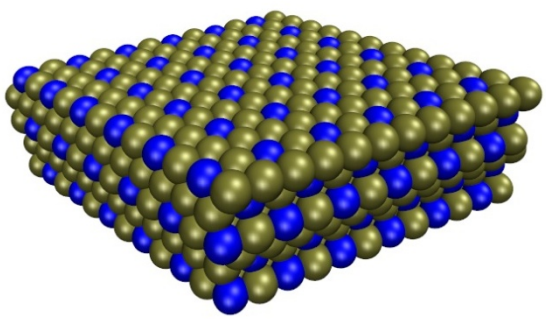

Figure: $Pt_3Ni(111)$ surface

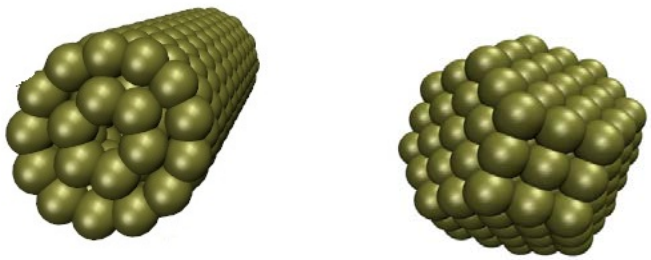

Figure: (6,6)@(13,13) MWPtNT nanotube and 2nm Pt_{201} cluster

Study the influence of alloying component **concentration and distribution** on the **ORR activity** and **stability** in aqueous environment

Study the effect of **size and structure** of a nanomaterial on the ORR activity and stability in aqueous environment

$$\frac{1}{2}O_2 + * \rightarrow O*$$

$$O* + e^- + H^+ \rightarrow OH*$$

$$OH* + e^- + H^+ \rightarrow * + H_2O(l)$$

relative to the standard hydrogen electrode

$e^- + H^+(aq) = 1/2H_2(g)$

Metal Nanotubes

Magic "structure" and conductance - nanoelectronics

Au, Ag nanotubes less then 2nm thickness have been synthesized by an electron-beam technique in an UHV-TEM

PtNT: Rolling-up Pt(111) sheet to form a tube

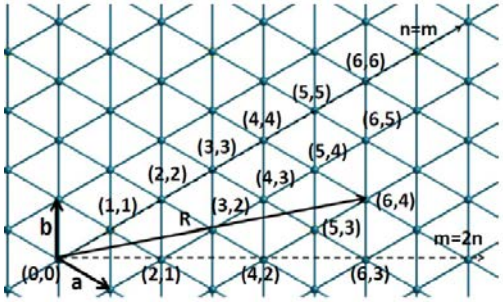

Roll-up →

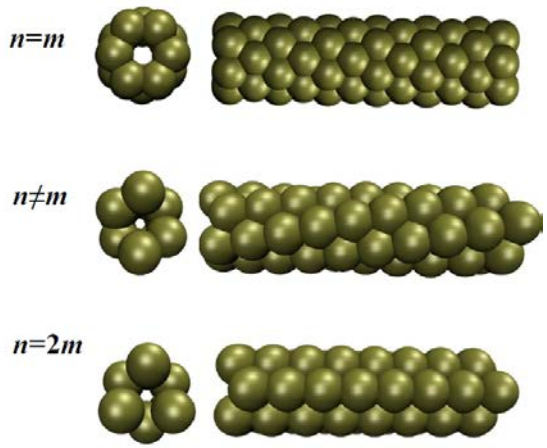

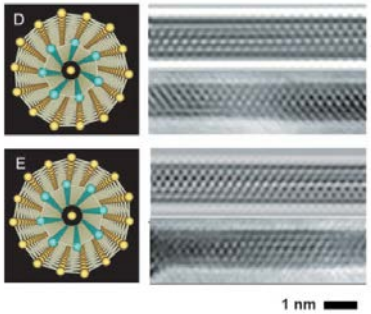

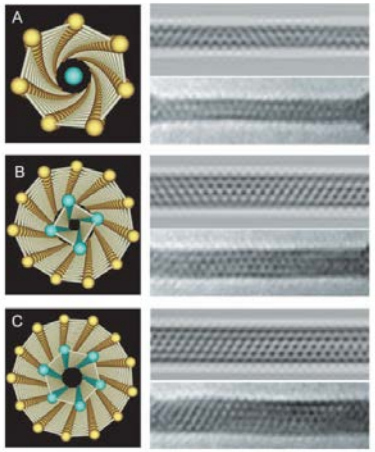

$$R = na + mb$$

$$r = \frac{\sqrt{2}a_c}{4\pi}\sqrt{n^2 + m^2 - nm}$$

a_c = 3.70- 3.85 Å

Kondo et al. Science, 289, 606 (2000)

Pt Nanotubes with Adsorbates

Pt nanotubes + oxygen

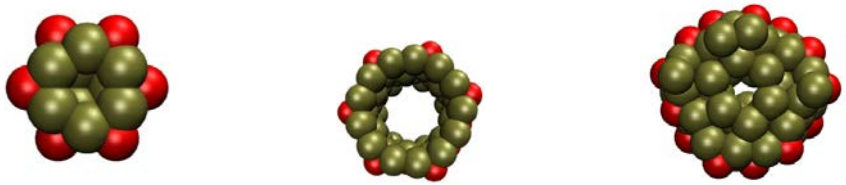

		0.25 ML		0.33 ML		0.5 ML	
		E_{ad}	ΔU_f	E_{ad}	ΔU_f	E_{ad}	ΔU_f
	Pt	-4.42	0.00	-4.25	0.00	-4.07	0.00
	(6,3)	-4.72	-0.15	-4.52	-0.14	-4.50	-0.22
$\approx$ 0.5 nm	(6,4)	-4.70	-0.14	-4.31	-0.03	-4.44	-0.19
	(6,6)	-4.72	-0.15	-4.41	-0.08	-4.46	-0.20
	(12,6)	-4.29	+0.07	-3.98	+0.14	-3.96	+0.06
	(12,8)	-4.29	+0.07	-4.03	+0.11	-4.00	+0.04
$\approx$ 1nm	(12,12)	-4.18	+0.12	-3.94	+0.16	-3.97	+0.05
	(13,13)	-4.14	+0.14	-3.90	+0.17	-3.92	+0.08
	(6,6)@(13,13)	-4.05	+0.19	-4.21	+0.02	-4.06	+0.05

Adsorption energies in eV and a shift in equilibrium adsorption potential in V for oxygen on the fcc site for different nanotubes and coverages

Pt nanotubes + hydroxyl

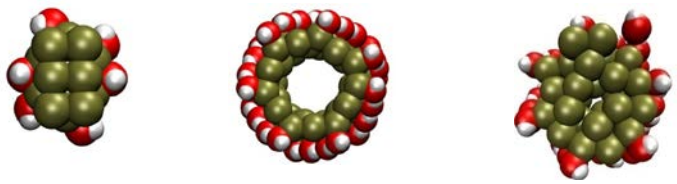

		0.25 ML		0.33 ML		0.5 ML	
		E_{ad}	ΔU_f	E_{ad}	ΔU_f	E_{ad}	ΔU_f
	Pt	-2.88	0.00	-2.92	0.00	-3.09	0.00
	(6,3)	-3.70	-0.82	-3.47	-0.55	-3.76	-0.67
$\approx$ 0.5nm	(6,4)	-3.60	-0.72	-3.35	-0.43	-3.69	-0.60
	(6,6)	-3.54	-0.66	-3.54	-0.62	-3.52	-0.43
	(12,6)	-2.92	-0.04	-2.98	-0.06	-2.73	+0.36
	(12,8)	-2.89	-0.01	-2.98	-0.06	-2.73	+0.36
$\approx$ 1nm	(12,12)	-2.89	-0.01	-2.97	-0.05	-2.91	+0.18
	(13,13)	-2.83	+0.03	-2.87	+0.03	-2.85	+0.24
	(6,6)@(13,13)	-3.07	-0.19	-3.13	-0.21	-3.20	-0.11

Adsorption energies in eV and a shift in equilibrium adsorption potential in V for hydroxyl on the top site for different nanotubes and coverages

Pt Nanotube Reactivity Behavior

- Smaller nanotubes (~0.5 nm) bind oxygen/hydroxyl more strongly than Pt(111)
- Larger nanotubes (~1 nm) bind oxygen/hydroxyl comparable or weaker than Pt(111)
- Reduced ORR overpotential – SWPtNT with a diameter > 1nm
- Control size/chirality – fine tuning of reactivity → separation of metal nanotubes by geometric specification or size
- All studied nanotubes more susceptible to electrochemical dissolution than Pt(111) – potential corrosion problem

Calculated surface Pourbaix diagrams for Pt nanotubes vs Pt bulk (dashed)

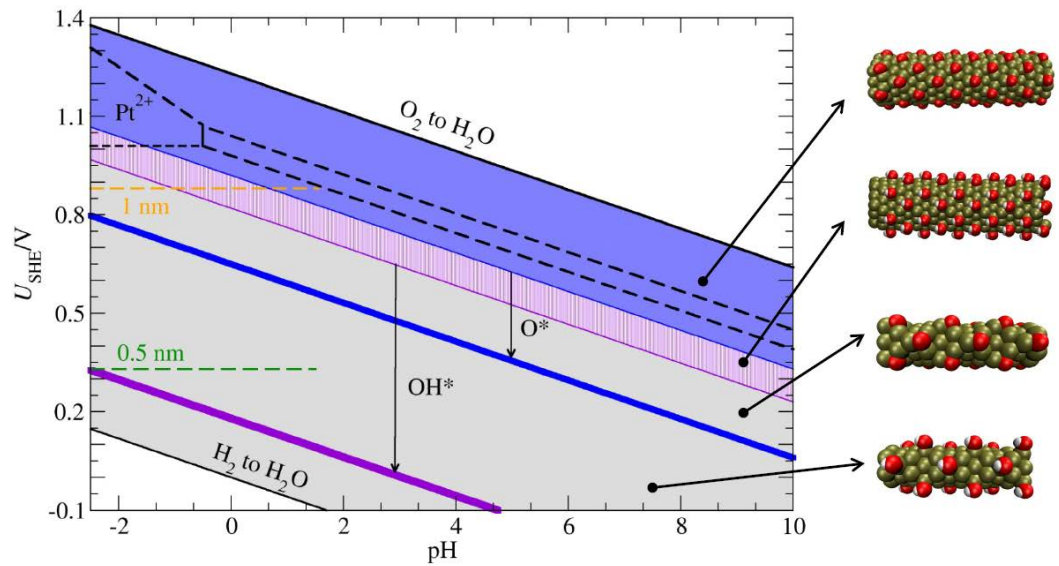

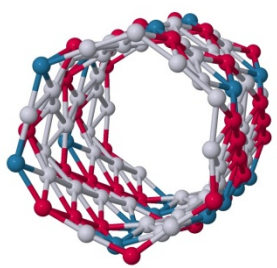

reaction	$M_N(\text{tube}) \rightarrow M_{N-1} + M$	ΔE/eV	ΔU_{corr}/V
	Pt(111)	6.55	0.00
	(6,3)	3.63	-1.46
≈ 0.5 nm	(6,4)	5.16	-0.70
	(6,6)	5.27	-0.64
	(12,6)	5.71	-0.42
	(12,8)	5.25	-0.65
≈ 1 nm	(12,12)	6.05	-0.25
	(13,13)	6.29	-0.13
	(6,6)@(13,13)	5.98	-0.27

Modeling: Catalyst Microstructure

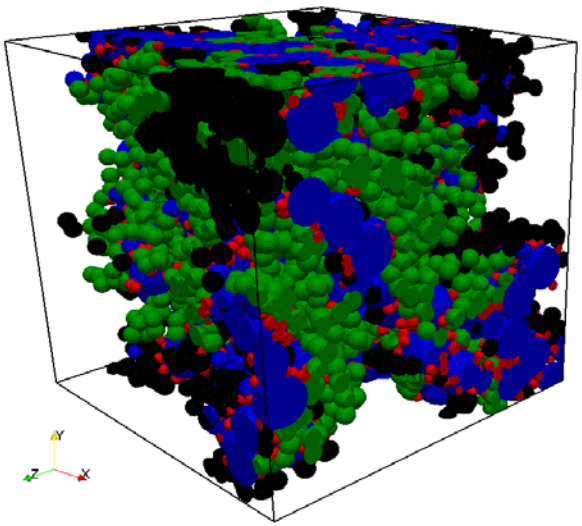

Simulation of Catalyst Polarization:

- Effect of platinum dispersion
- Transport effects due to ionomer and phase percolation
- Composition and Effective properties

Model Inputs:

- Particle size, shape and distribution (support, catalyst)
- Ionomer chain size and shape (assumed spherical ball)
- Layer Composition and loading
- Layer thickness or porosity

Ionic potential in y-dir

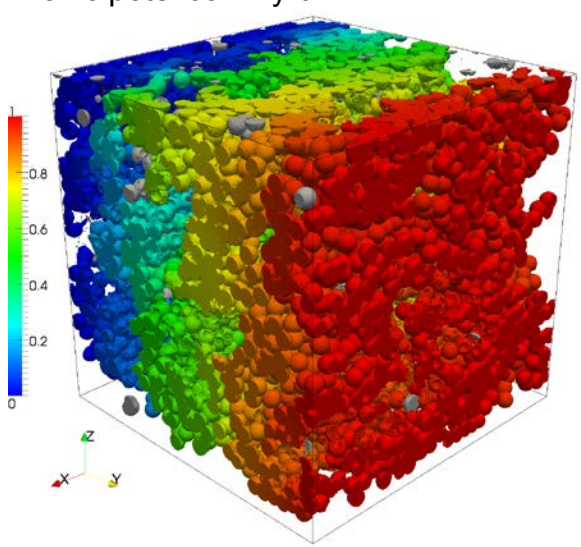

Effective properties of x, y, z-directions are evaluated by computational grid studies

Effective electron/ion conductivities, gas diffusivity as well as tortuosity factor are calculated as follows:

$$\nabla \cdot (\alpha \nabla \phi) = 0,$$

$$\frac{\alpha^{eff}}{\alpha} = \frac{\int \frac{\partial \phi}{\partial n} dS}{\frac{\Delta \phi}{L} A_s}$$

$$\tau = \frac{\epsilon_{phase}}{\frac{\alpha^{eff}}{\alpha}}$$

Microstructural Modeling

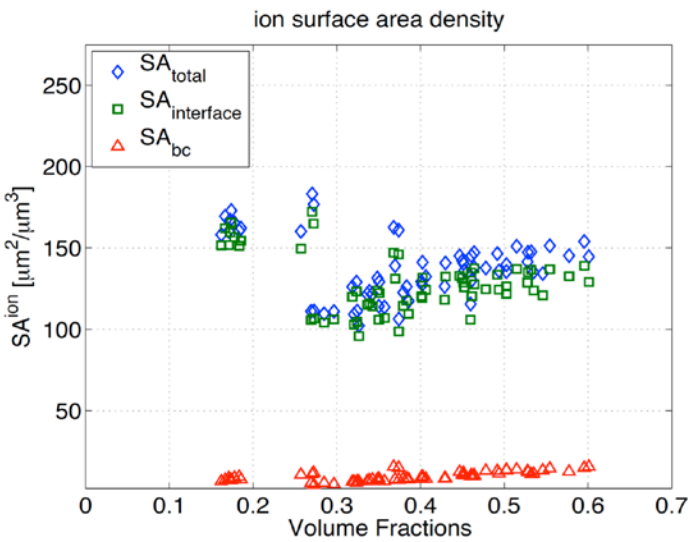

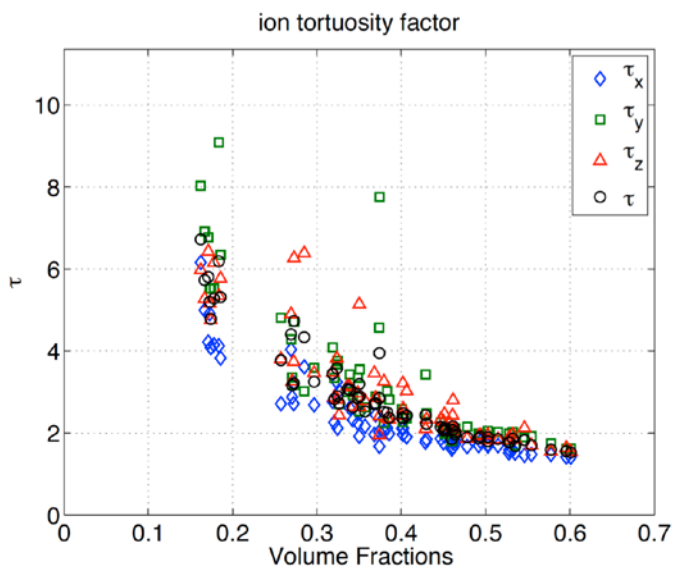

- The surface area of ionomer to gas phase changes slightly with volume fraction.
- Tortuosity shows some scatter, predominantly at lower volume fractions.
- Tortuosity declines, approaching a value a little less than two at high volume fractions.

•Established mesh requirements for estimation of effective properties

•Initial correlations developed for effective transport properties (conductivity) of proton/electron phases and (diffusivity) pore phase.

•Investigated correction factor (tortuosity) for each phase as a function of composition

•Performance simulations have been run on the baseline catalyst

•Reporting of geometric based current (based on sample adjustment) vs. Reporting per unit Pt surface

•Correlation to observed transport limitations

•Whether the lower catalyst performance (observed) is due to TOR or inherent transport limitations

Pt Nucleation and Growth on Carbons

- High dispersion i.e. small particles are needed to improve Pt utilization
- As particles become smaller, they become more unstable
- High Pt to C ratios improve F.C. performance; thinner electrode layer -better mass transport
- High Pt/C ratio requires more nucleation sites
  - Increase C surface area increases nucleation sites but decreases stability to oxidation
- Study nucleation and growth by EXAFS, TEM and EDS
- Two Pt particle formation mechanisms suggested from $PtCl_6^{=}$ precursor:
  - Strong Electrostatic Adsorption and Support Pt Reduction Dry Impregnation
- Alternate Method Ethylene Glycol Reduction Method
- Use two Carbons with differing surface areas Vulcan ~ 250 m^2/g , Norit 1000 m^2/g

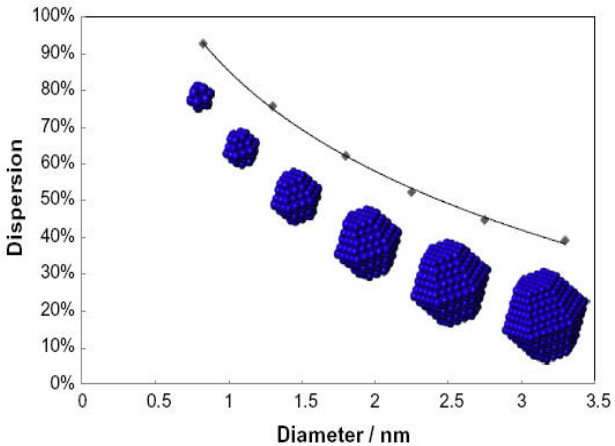

Dry Impregnation-add Pt solution drop wise
Strong Electrostatic Adsorption-add Pt and Carbon in solution while controlling the pH

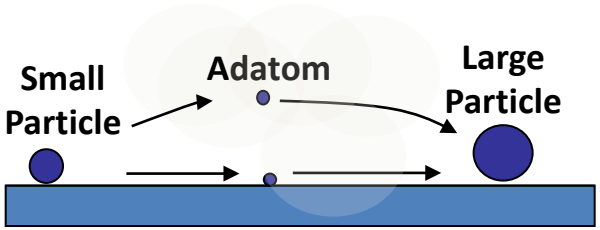

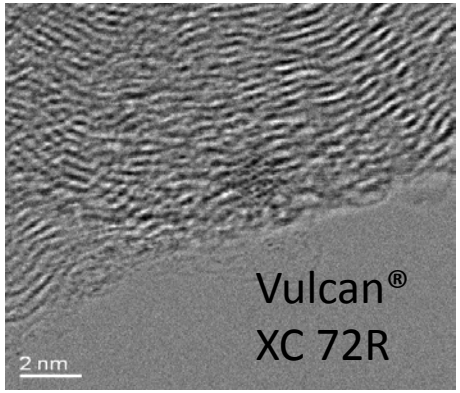

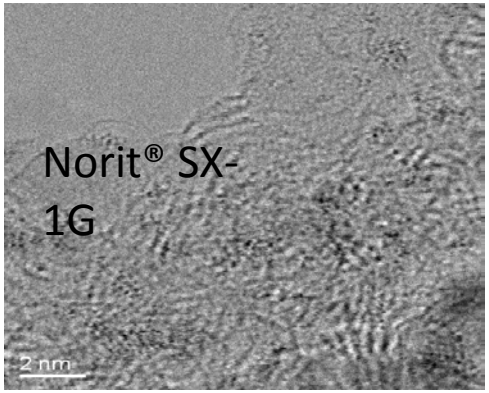

Electrostatic Adsorption: Vulcan and Norit

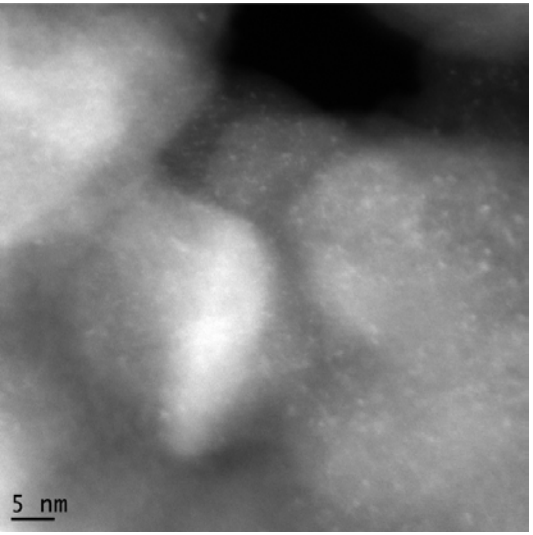

HRTEM Average Diameter=0.6nm

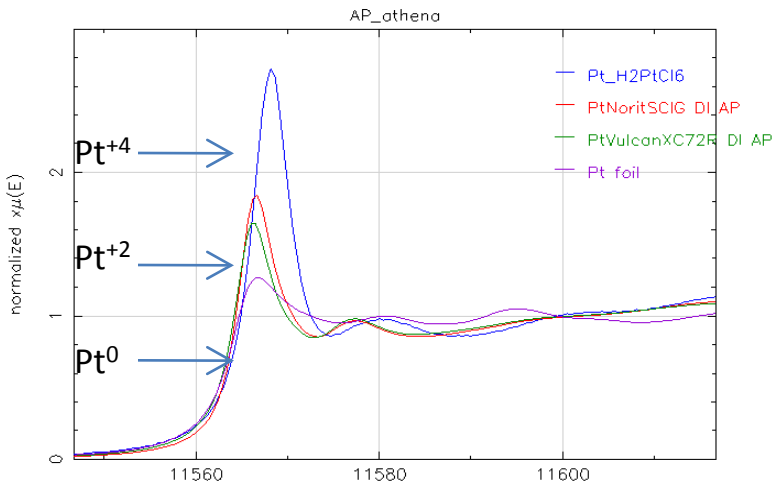

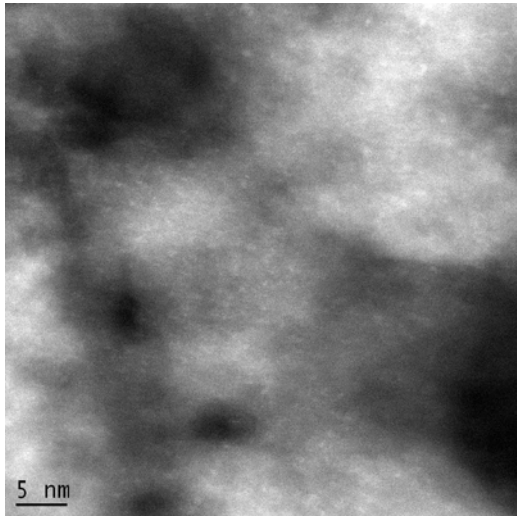

HRTEM Average Diameter=0.3nm
Smaller pores=smaller particles

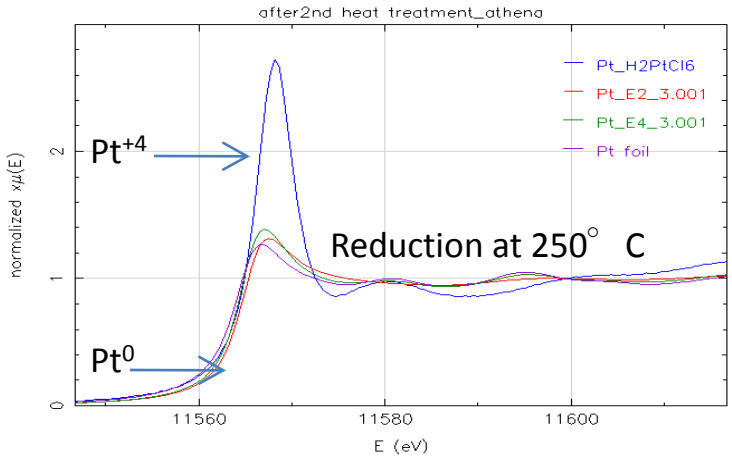

Pt^{+4} appears to already be reduced to Pt^{+2} once the solution makes contact with the support while further reduction occurs after heat treatments in hydrogen

Dry Impregnation: Vulcan and Norit

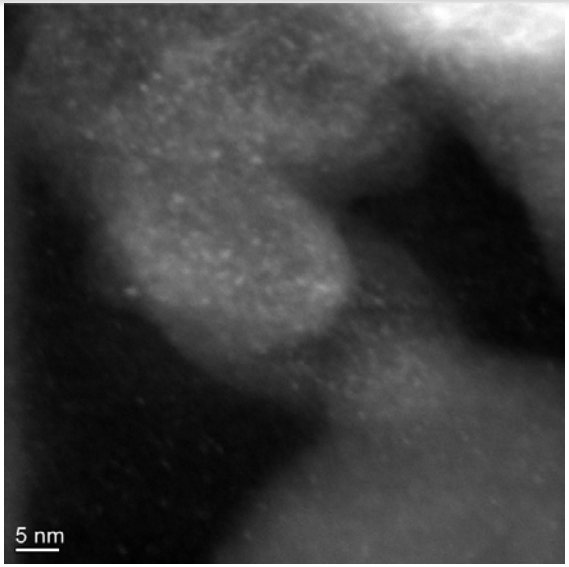

Pt on Vulcan
Average Diameter=0.9nm

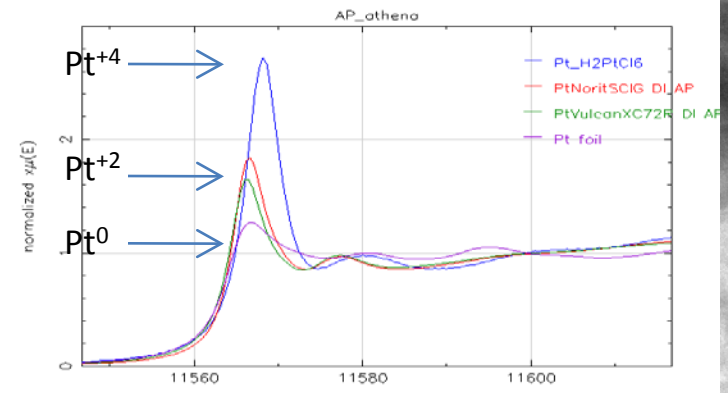

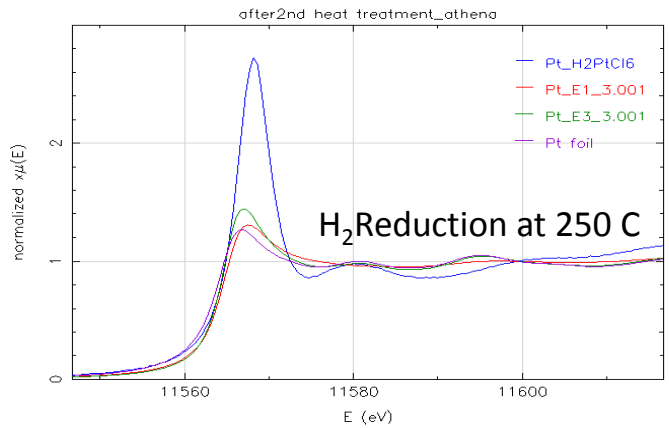

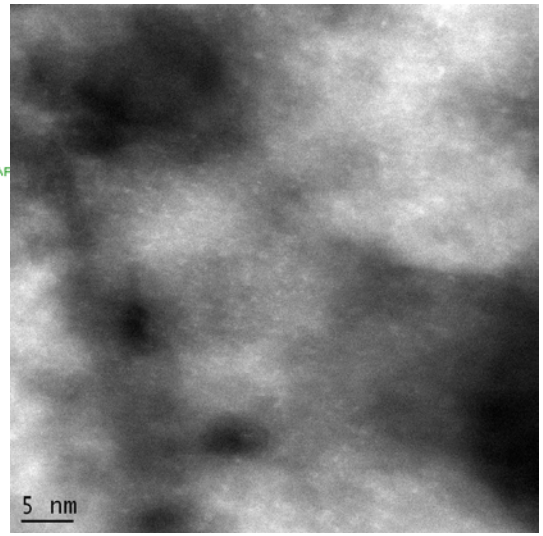

On Norit, Pt particles are homogeneously dispersed, avg. size ~0.3nm

- Vulcan had a larger Pt particle size compared the Norit carbon, also the Pt did not appear to adsorb on the larger spherical carbon particles
- XANES behavior the same as SEAS method

XANES Experiments Using Ethylene Glycol

- $H_2PtCl_6 \bullet 6\ H_2O$ in EG or Pt tetraamine salt
- Carbon in EG
- Mix the two and heat
- Add NaOH to get desired pH
- Then filter and dry

- Use the beam line to determine the state of the Pt before carbon is added to the solution
  - We know from previous experiments that the Pt reduces to +2 right after contacting the carbon
- Our experimental setup consisted of small tubes with solutions
  - 300µl of CPA for every 3ml of either EG or H_2O
  - Room temp, 50 C and 70 C measurements
- <u>No Pt reduction by ethylene glycol observed at 70 C</u>
- <u>Chloroplatinic acid: Pt Reduction occurs at 110 C</u>
- <u>Pt tetraamine: No Pt reduction at 125 C</u>

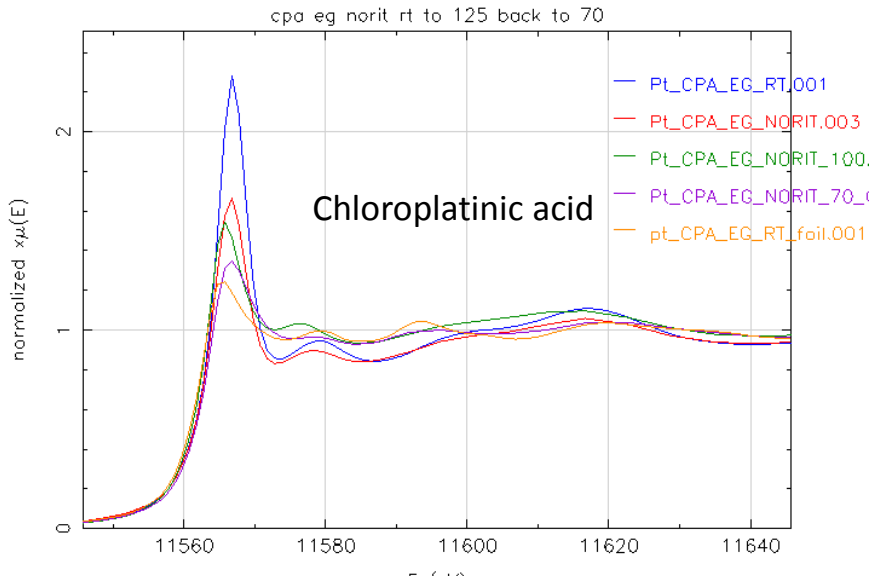

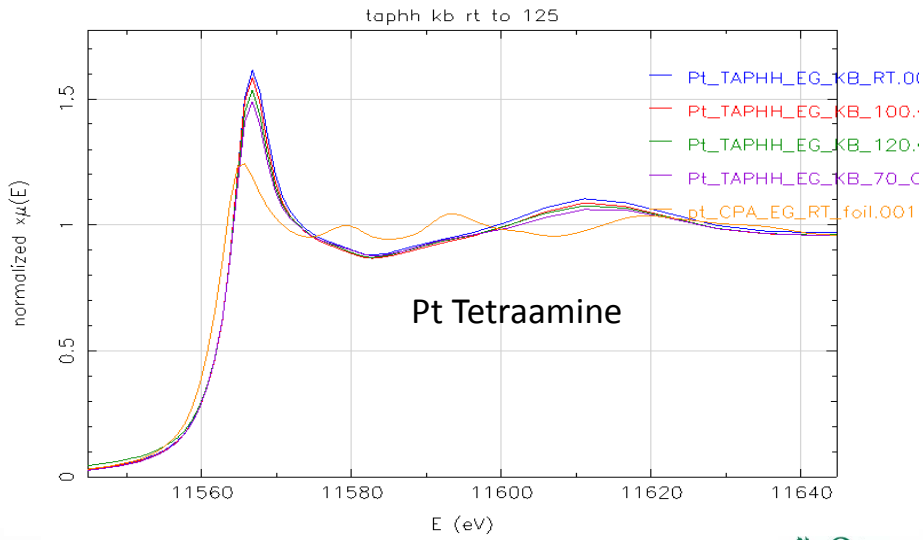

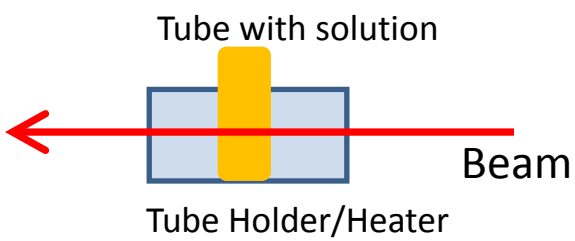

Pt Ceria Carbon Process For Oxygen Radical Scavenging Catalysts

High Surface Area Carbon Support by Steam Activation

Ceria/Carbon Bead
SA ~ 60 - 75 m^2/g

Ce/C Bead
SA ~ 250 m^2/g

Ce/C Powder
SA ~ 300 m^2/g

- Investigate nanoceria oxide (2-5nm) free radical scavengers for improved carbon support durability
- Study effects of M^+ doping on ceria radical scavenging activity
- Increase CePrOx/C support area to increase Pt dispersion with the introduction of high (>30%) Pt loadings

- Destroy radicals close to ORR catalyst surface
- Limit damage to carbon support

- Cl free Pt deposition:
  - Reduce Pt salt in ethylene glycol
  - ~ 130˚C for 3 h
  - tetra-amine platinum hydroxide
  - does at least as well as chloroplatinic acid (in our hands)
  - do not have to wash (if a small sample size)

Panagiotis Trogadas, Javier Parrondo, and Vijay Ramani
Electrochem. Solid-State Lett., Volume 11, Issue 7, pp. B113-B116 (2008)
12 nm ceria in ionomer ink

Pt Deposition on CePrOx/Carbon (cont.)

Pt-111117 – 30% Pt on steam activated $(CePr)O_2/C$

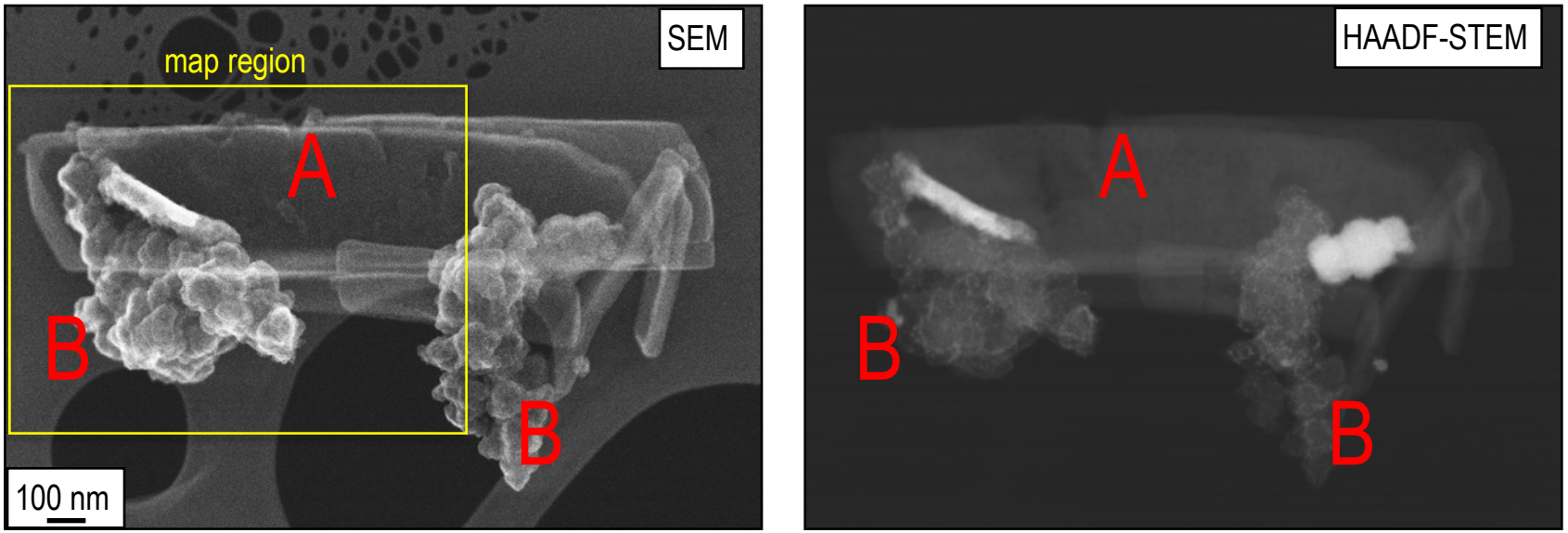

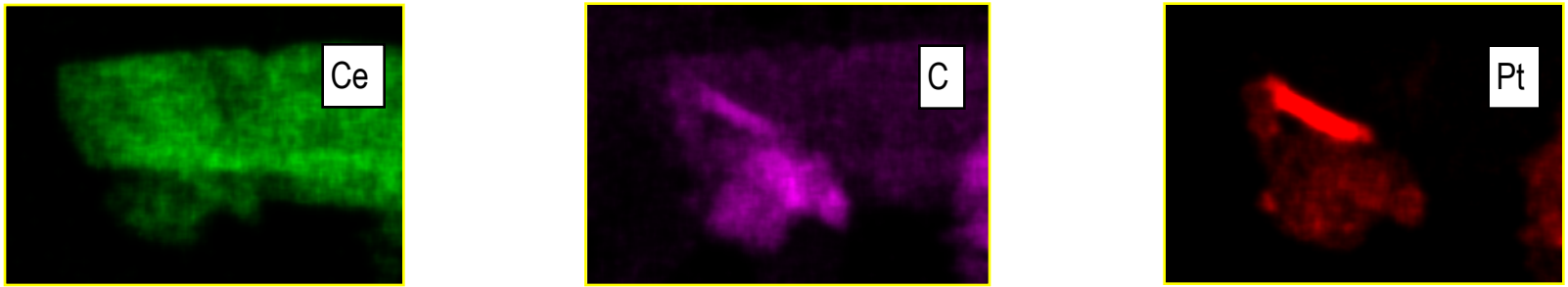

- Carbon removal is not uniform, substantially greater “activation” in certain regions results in C deficiencies
- Pt prefers the carbon even with the use of the Amine-EC process and Pt(II) precursors.
- Experiment: remove the C and see how the Pt disperses

Nano CePrOx Dispersion On TKK Catalyst Surface

- Direct Nucleation of Pt on Ceria- good dispersion but high electronic resistance so:
- Dispersed Ceria nanoparticles on surface of TKK carbon
- TEM shows they are individual Pt or $(CePr)O_2$
- SAD pattern indicates presence of both phases
- Large agglomerates of CePrOx powder, but about ½ the total is highly dispersed amongst the Pt
- RDE results similar to unseeded TKK
- AST testing proceeding at Ballard

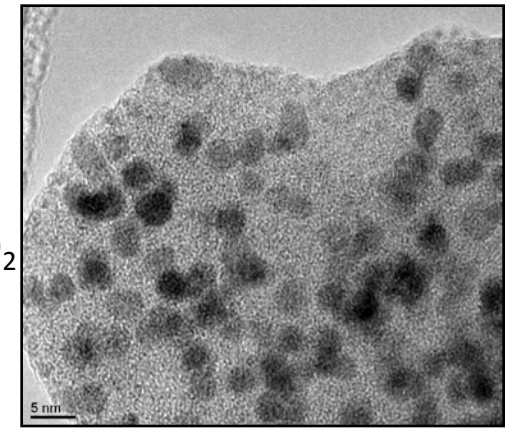

3nm Pt on Ceria grain by amine deposition

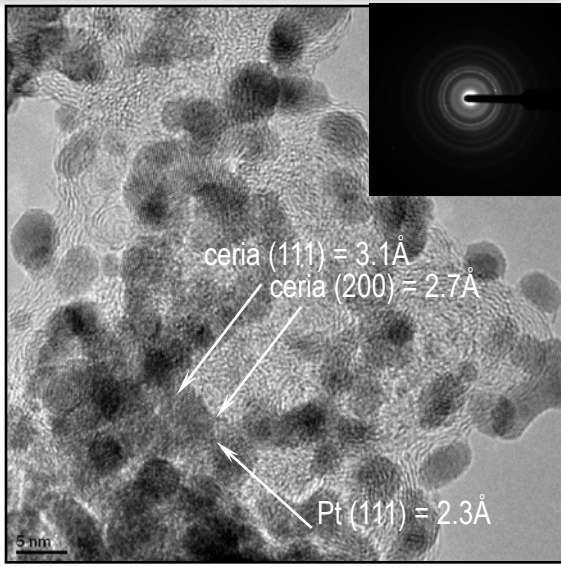

TKK Pt/C with Ceria nanocatalyst

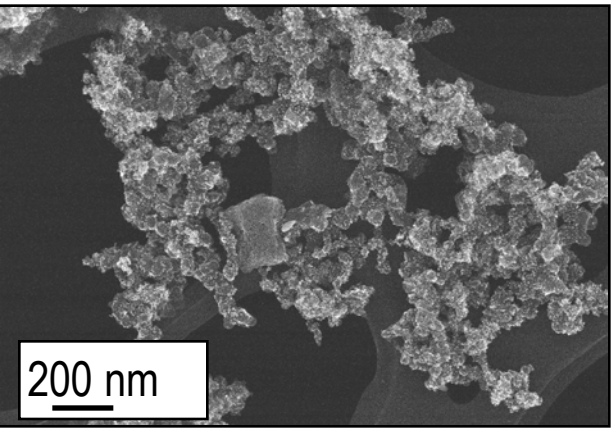

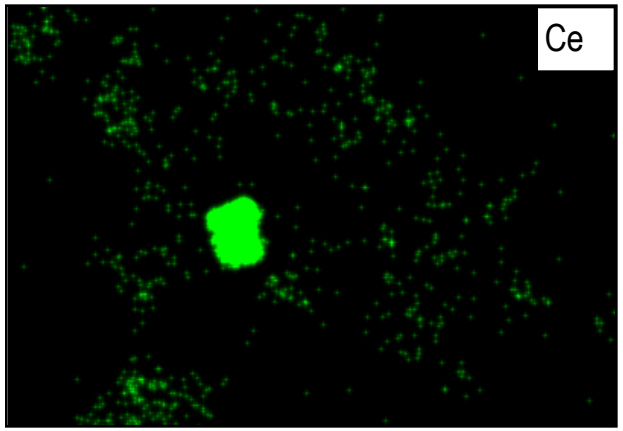

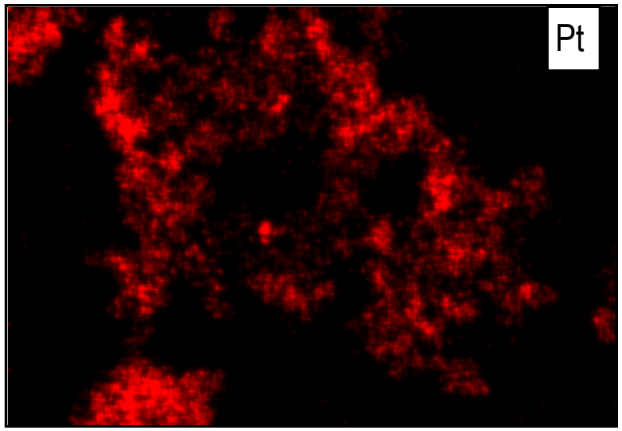

PtPd Nanoplatelet Catalysts

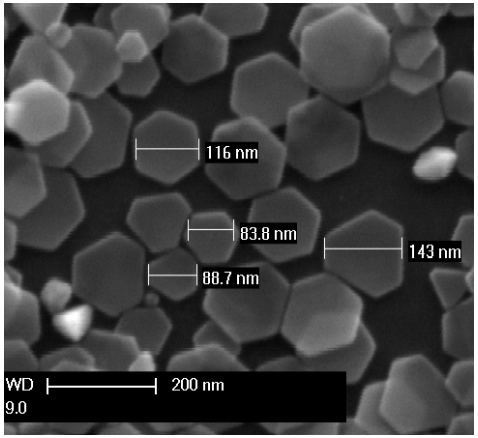

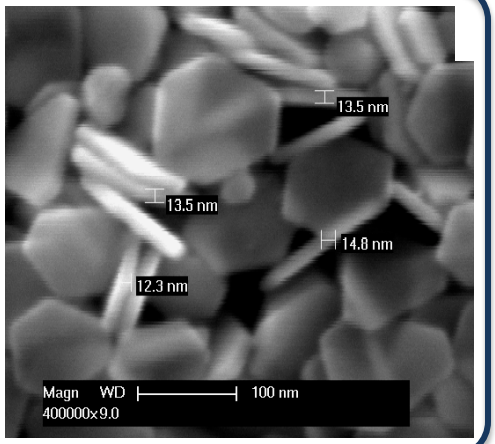

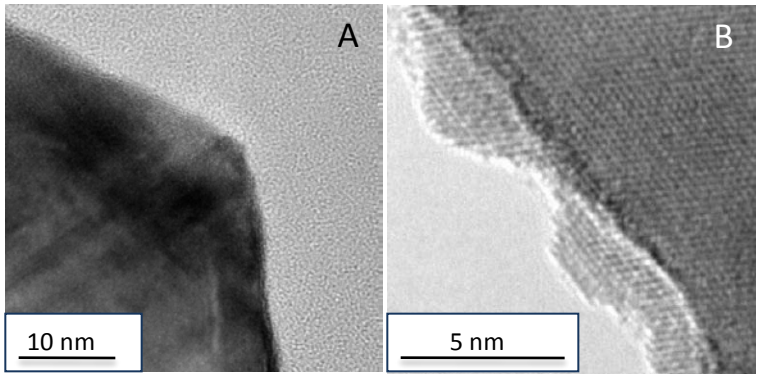

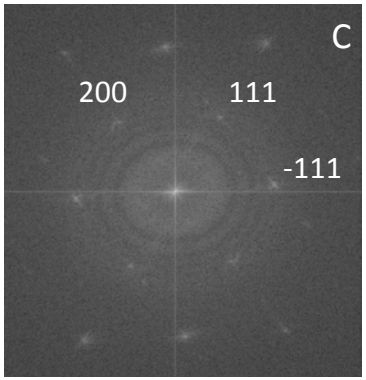

A) TEM

B) HRTEM

C) FFT Pattern

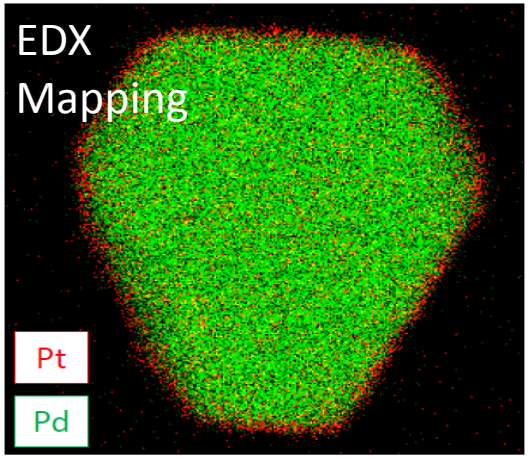

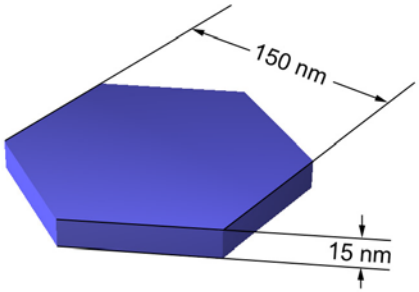

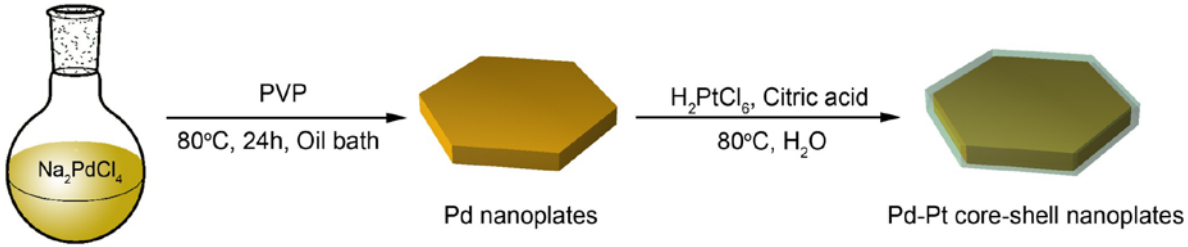

Activity and Durability of New Pt_3Y and Pt_3Sc Catalysts

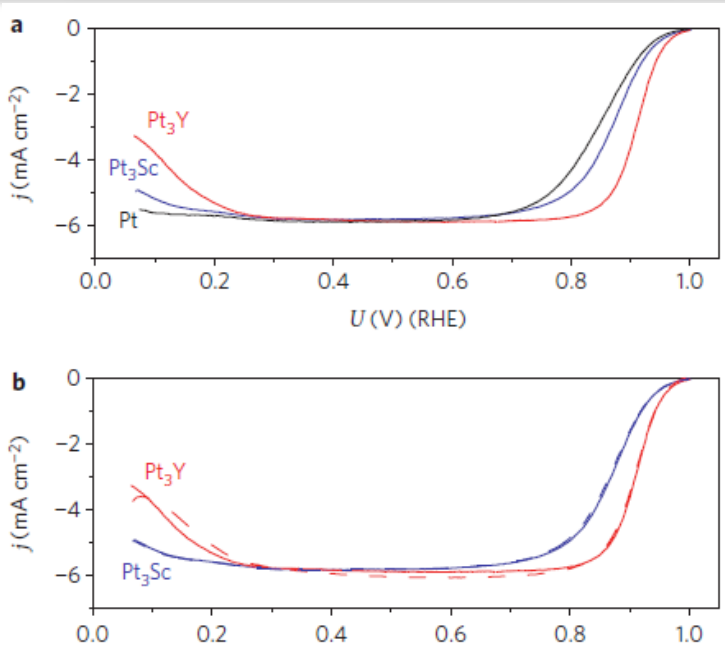

- Solid line: first steady cycle
- Dash line: after 90 minutes of cycling
- Both the specific activity and durability show an considerable improvement for bulk Pt_3Y and Pt_3Sc.

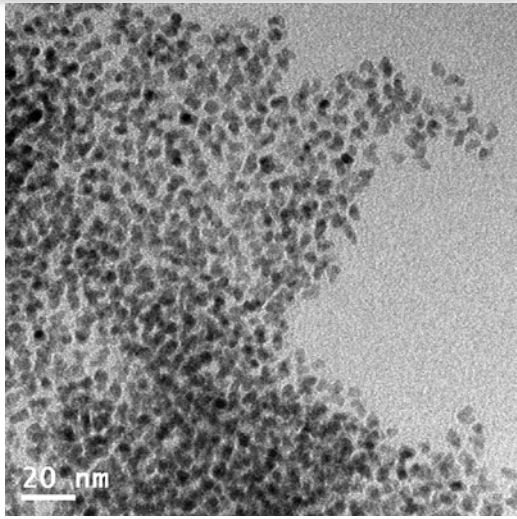

TEM images of as-synthesized Pt-Sc nanoparticles- Size distribution. 4-7 nm

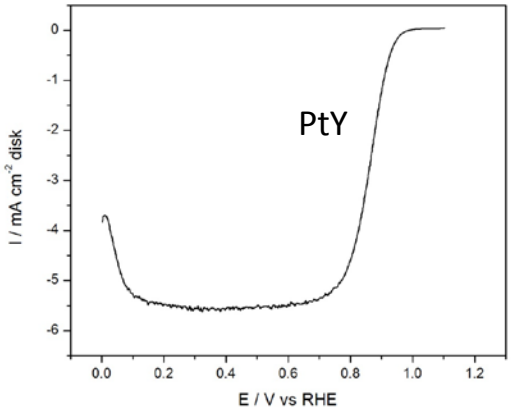

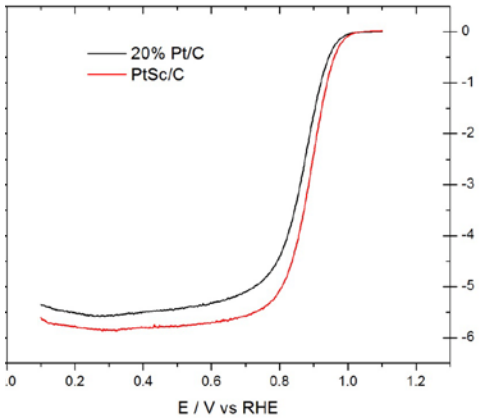

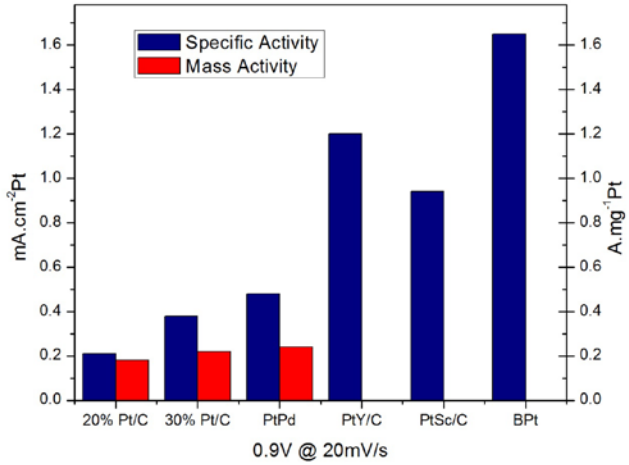

20 mV/s, 1600 rpm, $HClO_4$

Synthesis of PPY-Pt Catalysts

- Electrochemical synthesis of PPY-starch nanowires on a glassy carbon (GC) disk electrode using a polymerization charge of 75 mC (380 mC cm^{-2}), then:
  - Pyrolysis (ramp from 100 ºC to 1000 ºC at 5 ºC min^{-1} → 3 hours)
  - Morphology survives pyrolysis
  - Wire size decreases and more cross connection
- Pt deposition:
  - Impregnation with Na_2PtCl_6 and then thermal reduction at 200ºC in (6% H_2 / Ar) for 3 hours
  - Pt Sputtering under 2 mTorr (Ar) at 300 W
- Very uniform coatings achieved

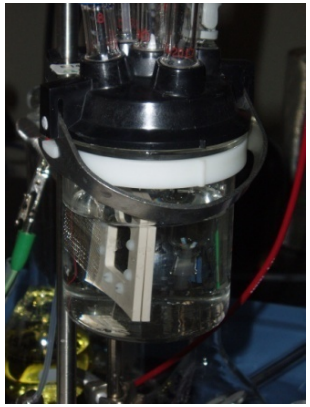

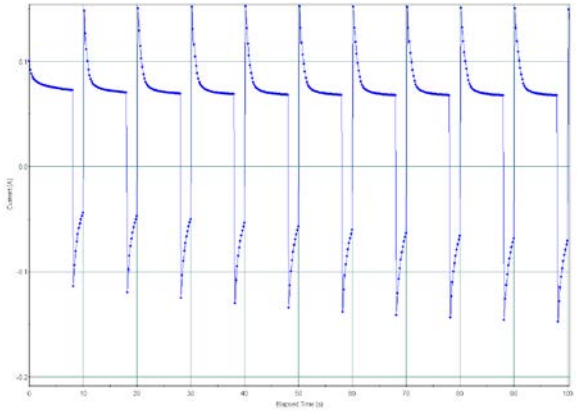

Electrochemical PPY Cell

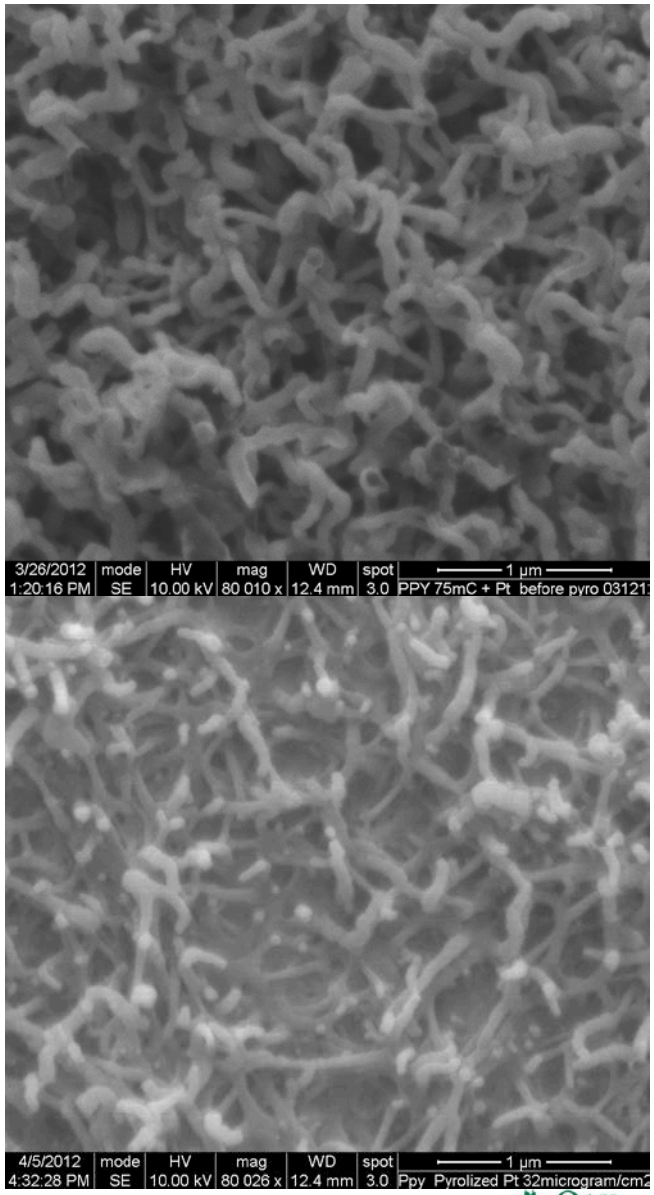

RRDE STUDIES 0.1 M $HClO_4$ (O_2) , 900 rpm , 5 mV s^{-1}

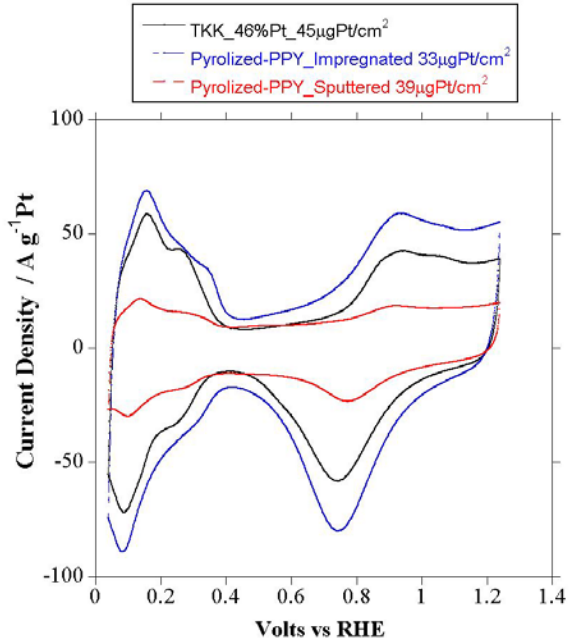

Catalyst	ESA (m^2 g^{-1})	Mass Activity at 0.9V (A g^{-1})	Surface Activity at 0.9V (μA cm^{-2})	E1/2 (V vs RHE)	H_2O_2 at 0.6V (molar %)
TKK (46% Pt)	72	59	82	0.894	1.0
PPY-Pt (Impregnated)	83	51	57	0.867	1.6
PPY-Pt (Sputtered)	29	44	143	0.867	0.9

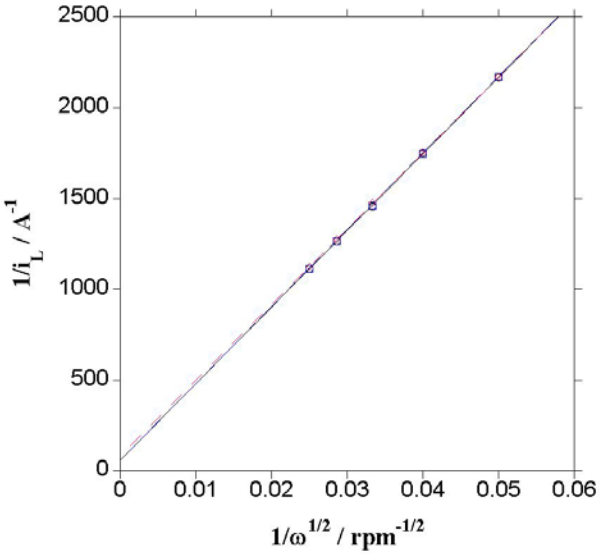

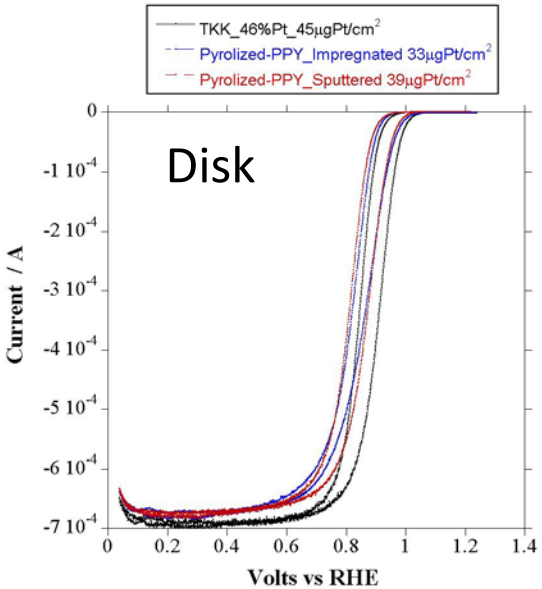

Pyrolized PPY Pt catalysts:

- Good activity and stability
- low peroxide generation

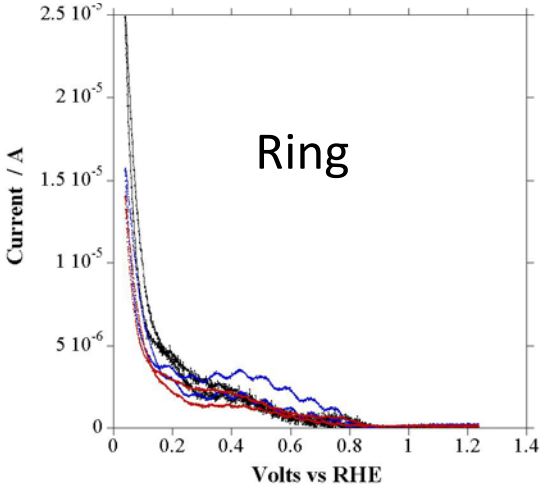

Fuel Cell ASTs

- BPS and DOE protocols have been characterized for the baseline catalyst.
- Results are consistent with expectations
  - Using the same (BPS) protocol (0.6-1.2V potential step), the MEAs with Pt loading of 0.1-0.3 mg/cm^2 showed similar %ECSA change and voltage degradation rate (up to 2100 cycles). However, the MEA with 0.1 mgPt/cm^2 showed much higher voltage degradation.
    - It also had higher Pt particle size increase (12 vs. 8 nm)
  - The higher the UPL reaches (1.2 *vs*. 1.0V), the faster cell voltage degrades and thinner the cathode catalyst layer thickness
    - Higher UPL also had higher Pt particle size increase (8 vs. 7 nm)
  - With the same UPL, Cell Voltage degrades slower if it is held at UPL than with potential steps
  - With UPL of 1.2V, the CL ionic loss and mass transport loss are significant
  - The 1.0V triangle cycling (DOE protocol) has the lowest degradation rate, and kinetic loss is the predominant factor of voltage degradation

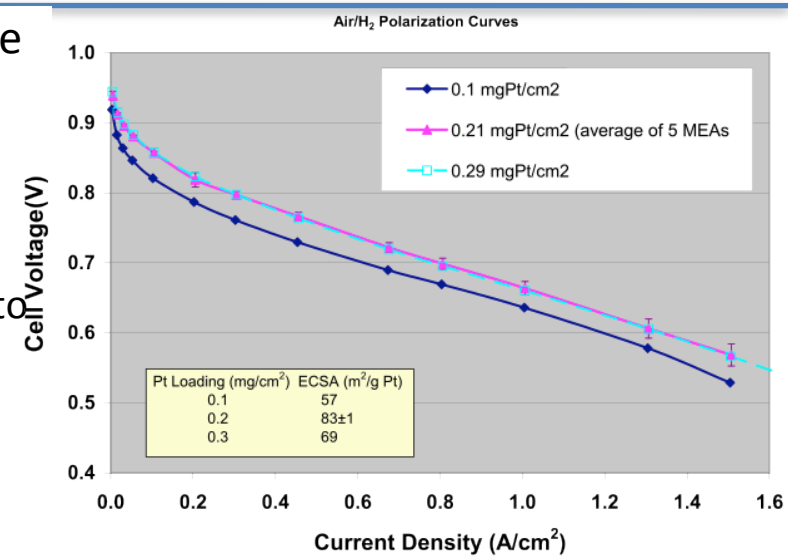

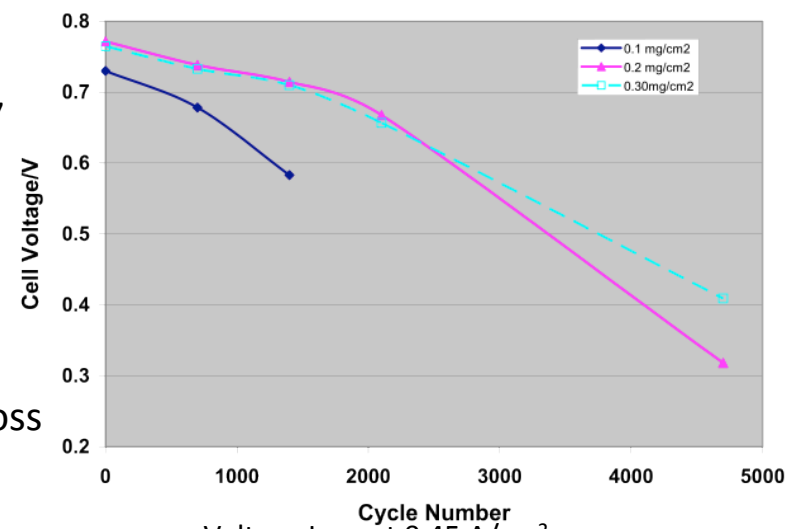

Voltage Loss at 0.45 A/cm^2, under BPS Protocol (0.6-1.2V)

Summary

- Modeling
  - DFT calculations providing insight into ideal alloy compositions, stable shapes
    - Lower binding energy for oxygen and hydroxyl on Pt nanotube surfaces
    - Show instability to collapse and of very small diameter Pt nanotubes
    - Predicts shifts in ORR
    - Small nanotubes susceptible to corrosion
  - Microstructure models developing
    - Will aid optimization of catalyst layers
    - Ground up optimization of catalysts layer shows the impact of tortuosity on ion transport
- Nucleation and growth study:
  - Shows all furnace carbons have similar nucleation site densities
  - Highlights the importance of increasing Pt nucleation site density on carbon surfaces
  - Pt VI to Pt II reduction on carbon surfaces very fast and critical step for deposition from Pt Cl salts
  - Ethylene glycol may not be acting as a reducing agent

- Synthesis and Characterization:
  - New Pt/carbon-ceria catalysts developed and characterized by XRD, HRTEM, Cyclic and RRDE voltammetry, and thermogravimetry
    - Show enhanced ORR activity over Pt-C
  - New Pt-Y and Pt Sc alloy catalysts developed and characterized by TEM and Cyclic and RRDE voltammetry
    - Show enhanced ORR activity over Pt-C
  - Pt on Pyrolyzed Polypyrrole characterized by TEM and Cyclic and RRDE voltammetry
    - Shows high activity for ORR and good stability

Milestones

- Synthesis of high activity catalysts
  - Pt –C / Ceria composite electrodes *completed Q5*
  - Pt Pyrolyzed Polypyrrole Nanowires *completed Q6*
  - Pt-Y and Pt-Sc *completed Q6*
- Electrochemical characterization of high activity catalysts
  - Pt-Y and Pt-Sc *completed Q6*
  - Pt –C / Ceria composite electrodes *completed Q5*
  - Pt Pyrolyzed Polypyrrole Nanowires *completed Q7*
- XRD characterization (Whole Profile Fitting) of new catalysts
  - Analysis of Pt-C/ceria catalysts *completed Q5*
- TEM of New Catalysts
  - HRTEM, STEM and SEM-EDS imaging of Pt Pd Nanoplatelets and Pt-C/Ceria catalysts *completed Q6*
- DFT modeling of Novel Pt shapes
  - Stability calculations of larger nanotubes *completed Q5*
  - ORR calculations on Nanotubes *completed Q6*
- Nucleation of Pt on supports study
  - EXAFS + TEM studies of Pt nucleation and growth completed Q7
- Microstucture Model Development

  Cathode Layer Microstructural Model extended to include tortuousity and Knudsen diffusion effects *completed Q6*

Future Work

- Pt/Ceria/C catalyst research
  - Pt-C/Ceria catalyst optimization- improve Pt dispersion
  - Pt/Ceria/catalyst neutron scattering
  - Scale up for fuel cell testing
  - Incorporation into catalyst layers and MEA optimization
  - Fuel cell performance and durability testing
- Pt/Polypyrrole catalyst research
  - Large batch synthesis and fuel cell testing
  - Calculate optimal MEA geometries
- Pt/Y,Sc nanoplate research
  - Decrease nanocrystal size
  - TEM and XRD characterization
  - Scale up for fuel cell testing
  - Incorporation into catalyst layers and MEA optimization
  - Fuel cell performance and durability testing
- Development of Models and Theory
  - DFT model extension to catalyst coated nanotube and nanowires
  - Microstructural Model Application to Novel catalysts
  - Model Validation

Acknowledgement

We gratefully acknowledge funding from the US DOE Office of Fuel Cell Technologies

Los Alamos NATIONAL LABORATORY EST. 1943 · BALLARD power to change the world · THE UNIVERSITY of NEW MEXICO · UNIVERSITY of DELAWARE · OAK RIDGE National Laboratory

Pt Nanotubes

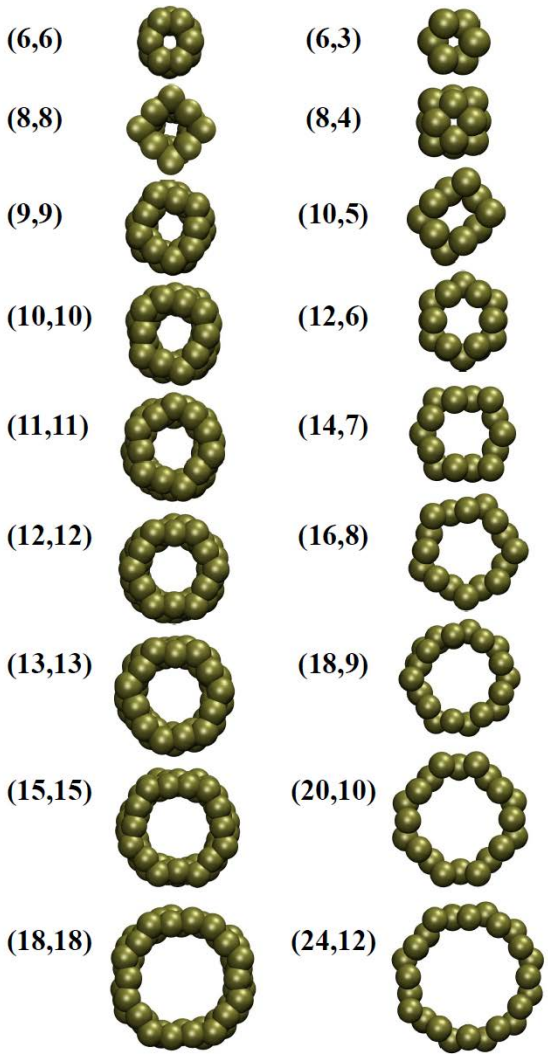

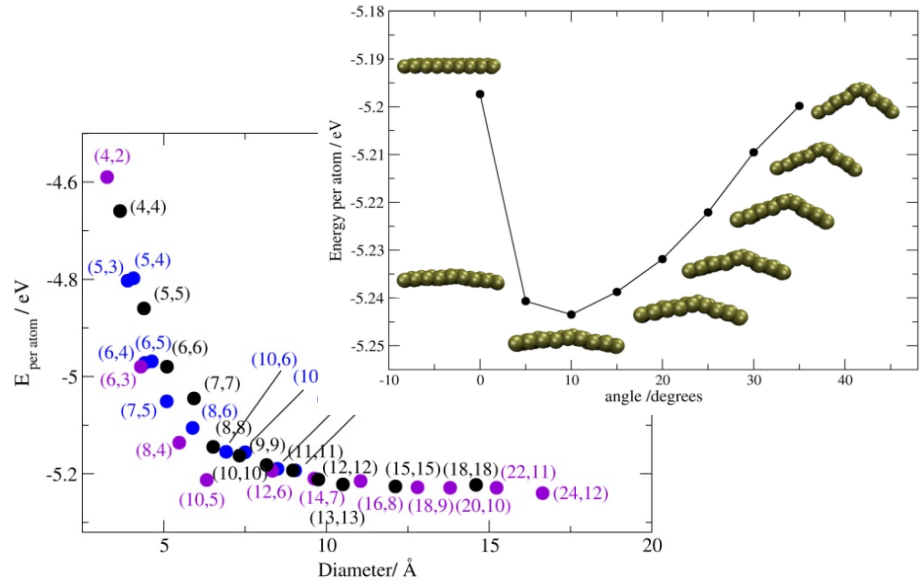

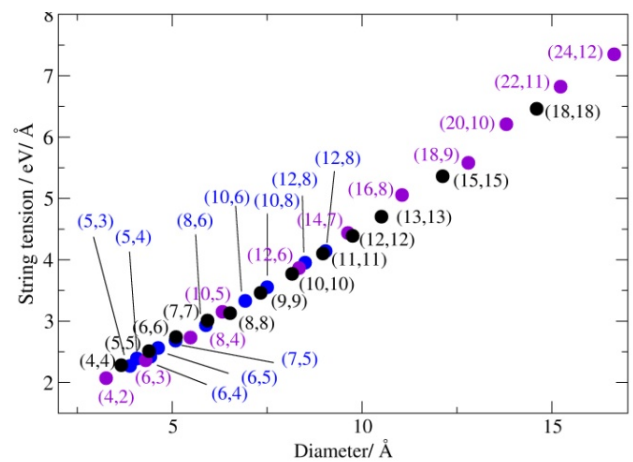

Methodology - Study of ORR mechanism

Reactions connecting different states of the metal surface(*) in the ORR mechanism

$$\frac{1}{2}O_2 + * \rightarrow O*$$

$$O* + e^- + H^+ \rightarrow OH*$$

$$OH* + e^- + H^+ \rightarrow * + H_2O(l)$$

relative to the standard hydrogen electrode

$e^- + H^+(aq) = 1/2H_2(g)$

Free gibbs energy of the reactions (Norskov et al. J. Phys. Chem. B 2006, 110, 21833)

$$\Delta G_{w,water} = \Delta E_{w,water} + \Delta ZPE + T\Delta S$$

$$\Delta G(U, pH, T = 298K) = \Delta G_{w,water} \underbrace{- eU}_{\text{bias effect}} + \underbrace{kT\ln(10)pH}_{\text{correction for the free energy of H+}}$$

Dissociative oxygen reduction reaction (ORR) mechanism

$$\frac{1}{2}O_2 + * \rightarrow O*$$

$$O* + e^- + H^+ \rightarrow OH*$$

$$OH* + e^- + H^+ \rightarrow * + H_2O(l)$$

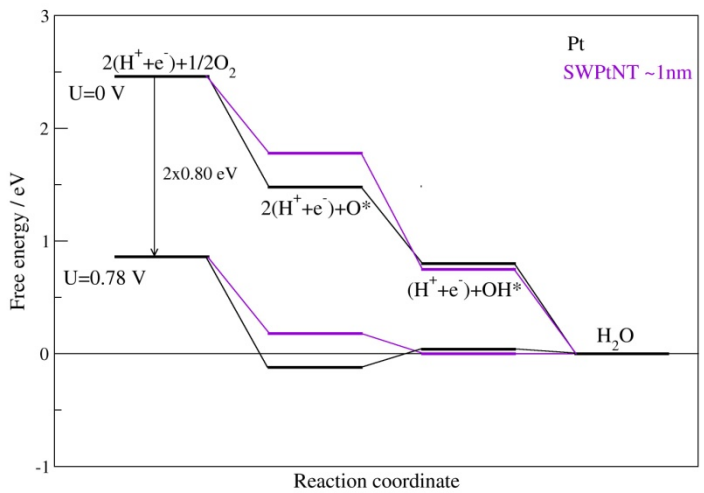

Figure: Free-energy diagrams for ORR over Pt(111) surfaces and SWPtNT for cell potentials U=0.80 V

In need for measurements – ORR curves

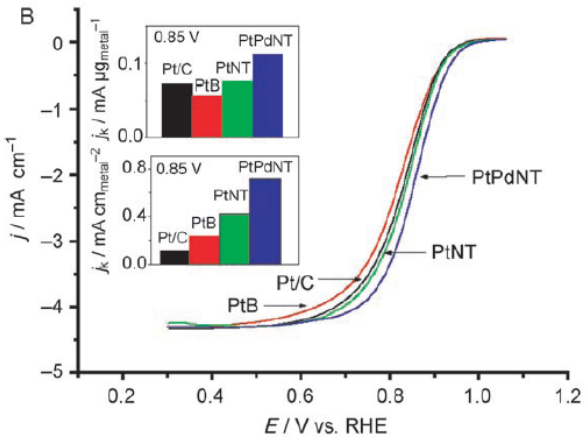

Chen et al., Angew. Chem. Ind. Ed. 2007, 46, 4060

PtNTs, d ~ 1nm- smaller ORR overpotential than Pt(111), up to 150 meV

Pt nanotubes – ab initio MD simulations in water

Aim (1) characterize change of atomic and electronic structure on solvation
(2) structure of water around curved surfaces - water-surface interface models

(6,6)

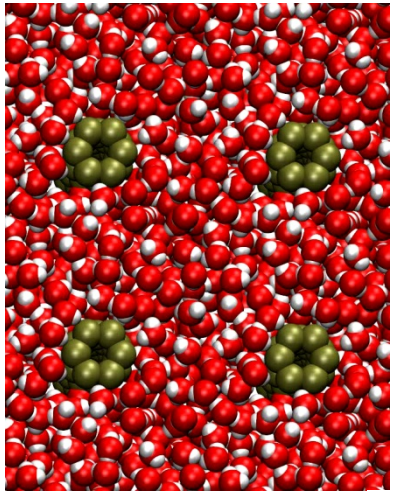

(13,13) SWPtNT

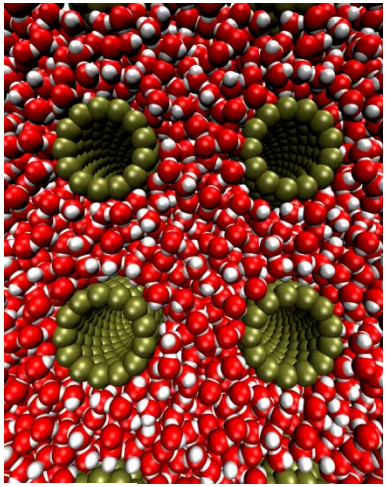

~800 atom cell, 1300 MD steps in 24h, 480 processors, average ~1min/step

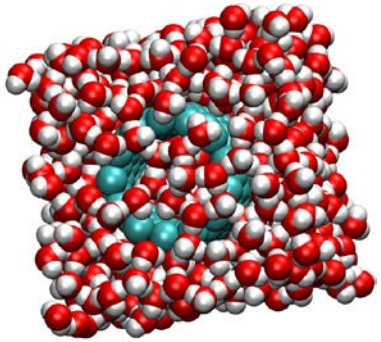

20 Å length tube, d=10.9 Å in a 30 Å length simulation box

bigger tubes accommodate water and ORR intermediates

Generation of Supported Catalyst

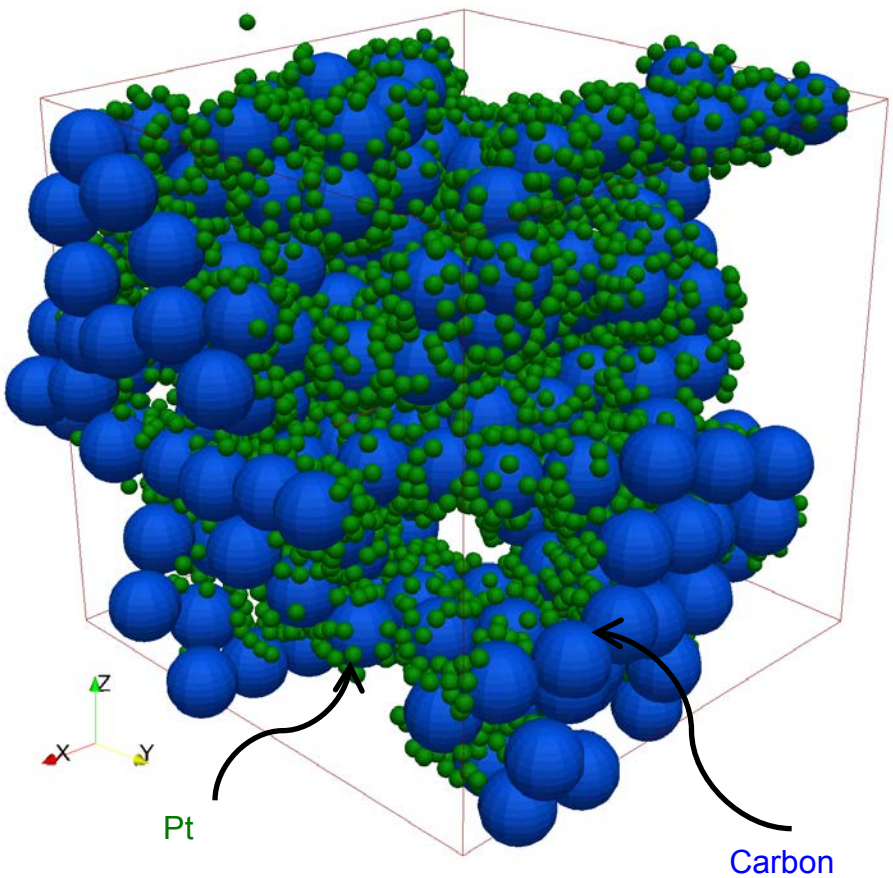

- A first Carbon particle is placed randomly in domain.
- Children particles are repeatedly placed randomly adjacent to their parent to form chained Carbon network.
- Overlaps are allowed to establish percolating network.
- Pt particles are deposited on Carbon network structure.

Generation of Ionomer Phase

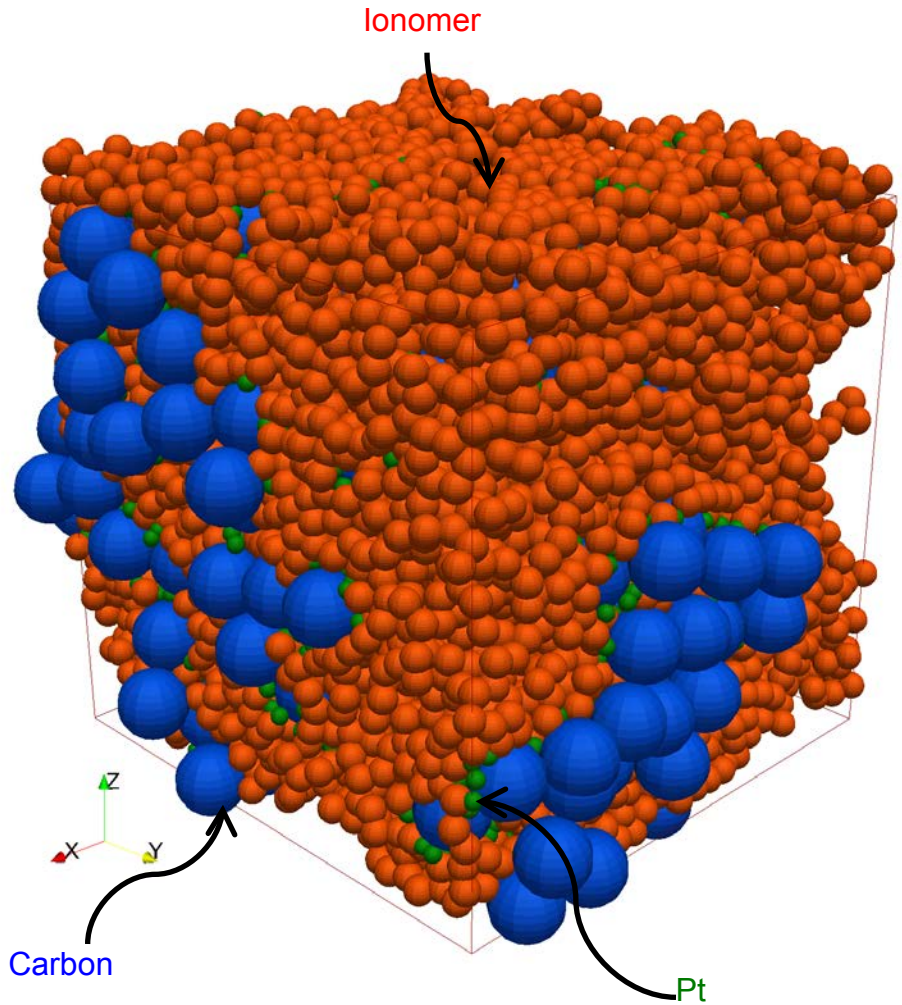

- Ionomer particles are deposited as sphere particles covering the Carbon+Pt sub-structures.
- Ionomer particles conform to Carbon/Pt particles they are placed on to serve reaction site.
- Ionomer particles establish their own percolating network.

Computational Discretization

- Surface triangulation of sample structure converted to discretized volume.
- Volume is discretized by cut-cell based unstructured grids using MicroFOAM1 based on OpenFOAM®2
- Discretized volume consists of 4 distinctive phases (Carbon, Pt, Ionomer, Pore)

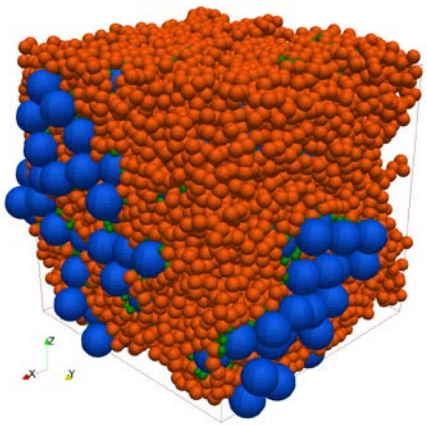

Pore space

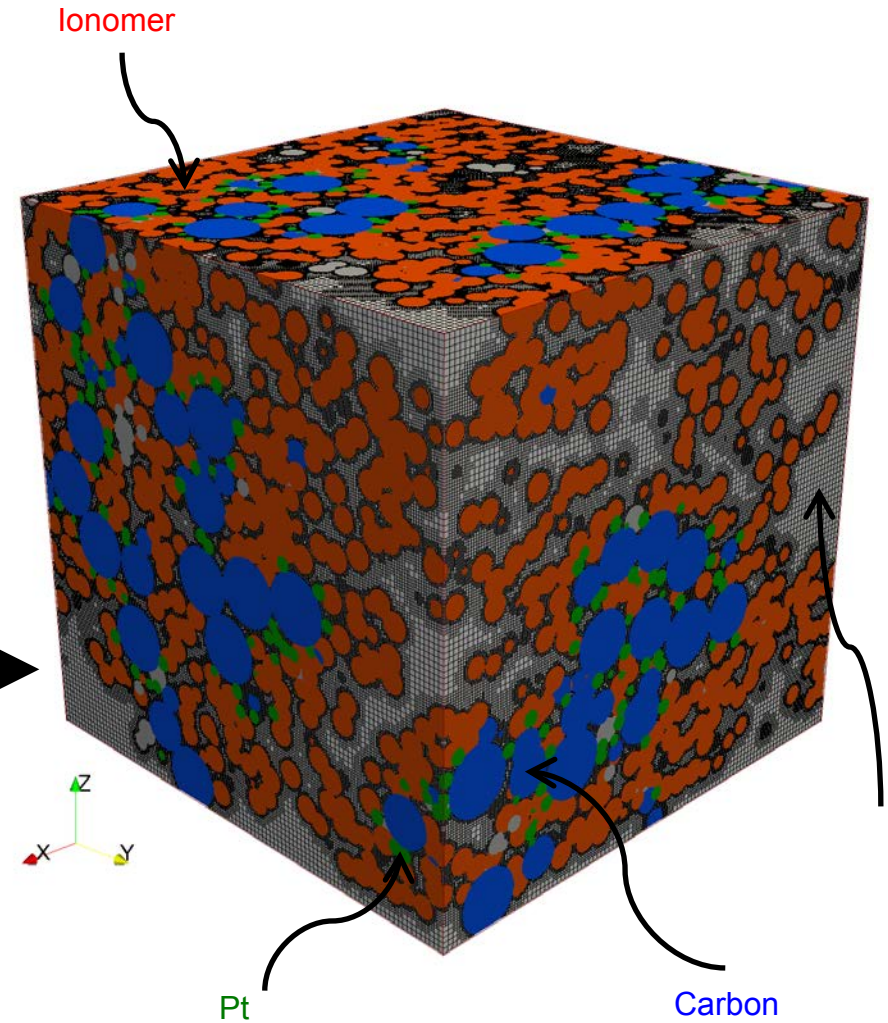

Grid Resolution

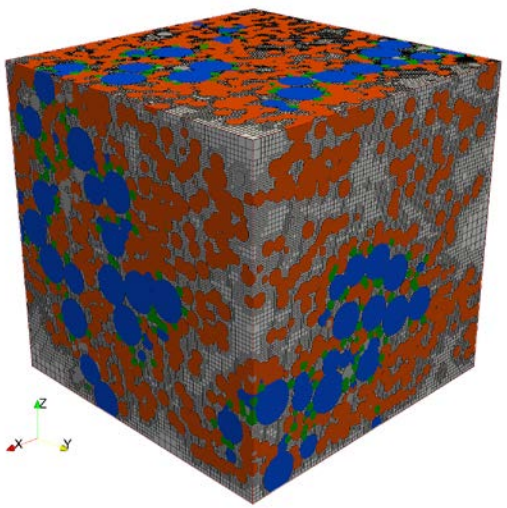

Electron: 0.88 millions
Ion : 1.28 millions
Pore : 1.48 millions
CPU cost: 0.44 hrs

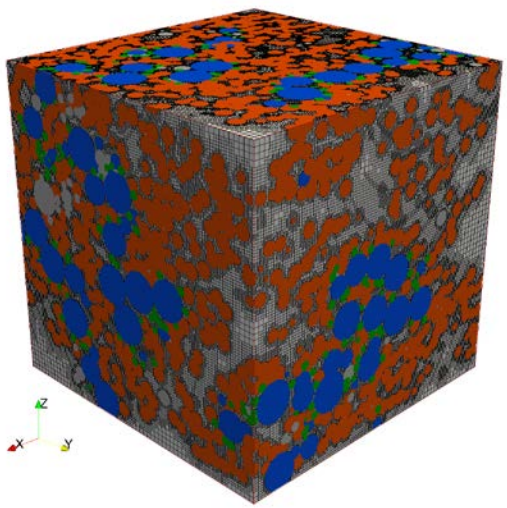

Electron: 2.58 millions
Ion : 4.12 millions
Pore : 4.52 millions
CPU cost 1.2 hrs

We will choose
this grid resolution
(based on grid
convergence results
In following slides)

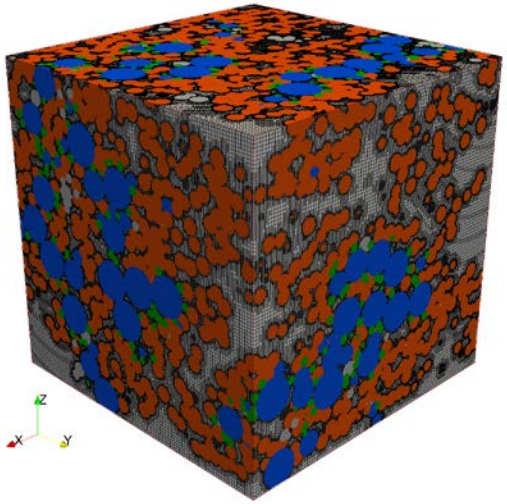

Electron: 5.44 millions
Ion : 8.95 millions
Pore : 9.56 millions
CPU cost: 2.5 hrs

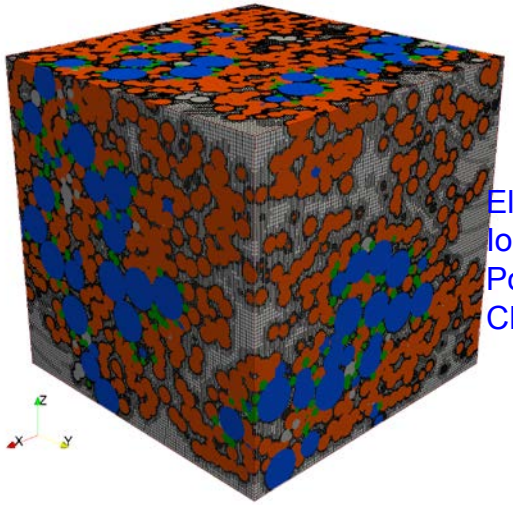

Electron: 9.65 millions
Ion : 15.98 millions
Pore : 16.77 millions
CPU cost: 4.2 hrs

Effective Properties

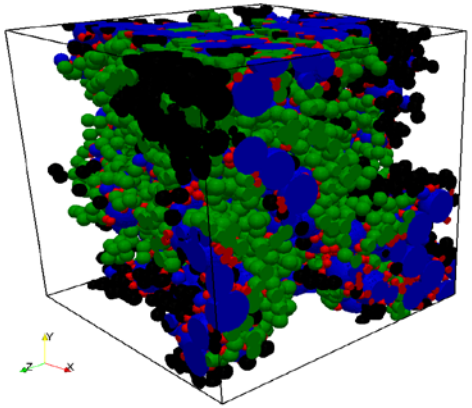

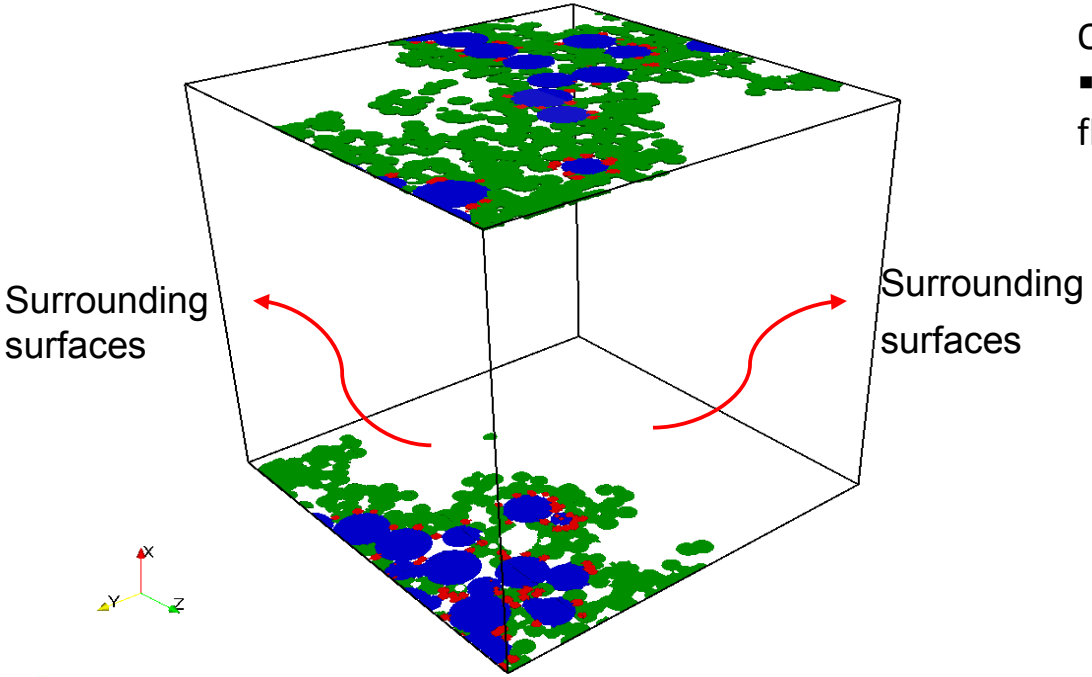

For the interfaces between each of the regions (carbon, platinum, ionomer and pore)

- Neumann Conditions are used when a phase is transporting
- A flux coupling is done when two phase regions are both "transporting"

On the top and bottom surfaces of the cube:

- Fixed values are set as boundary conditions.

On the sides of the cube:

- A symmetry condition is used to prescribe only flux in the through plane direction

Effective Properties

- Effective properties of x, y, z-directions are evaluated by computational grid studies
- Effective electron/ion conductivities, gas diffusivity as well as tortuosity factor are calculated as follows:

$$
\begin{aligned}
\nabla \cdot (\alpha \nabla \phi) &= 0, \\
\frac{\alpha^{eff}}{\alpha} &= \frac{\int \frac{\partial \phi}{\partial n} \, dS}{\frac{\Delta \phi}{L} A_s} \\
\tau &= \frac{\epsilon_{phase}}{\frac{\alpha^{eff}}{\alpha}}
\end{aligned}
$$

Electronic potential in y-dir

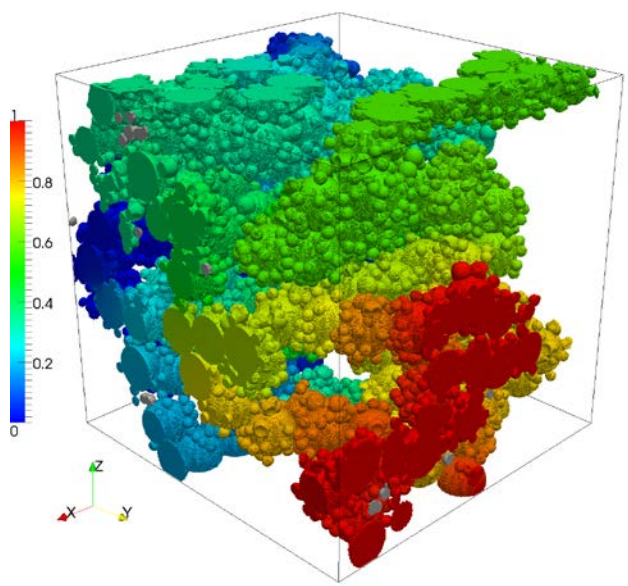

Ionic potential in y-dir

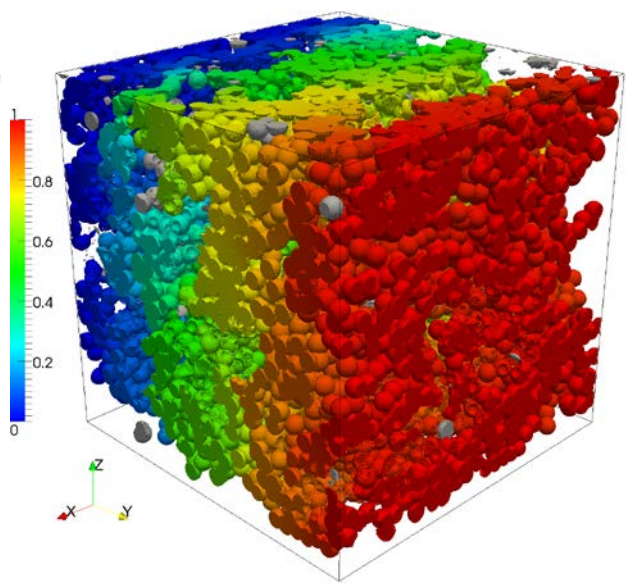

Gas phase potential in y-dir

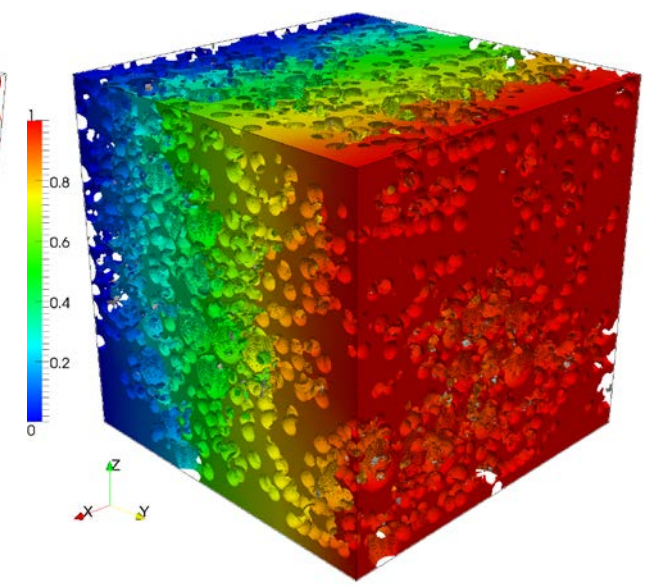

Effective Properties – Grid Study

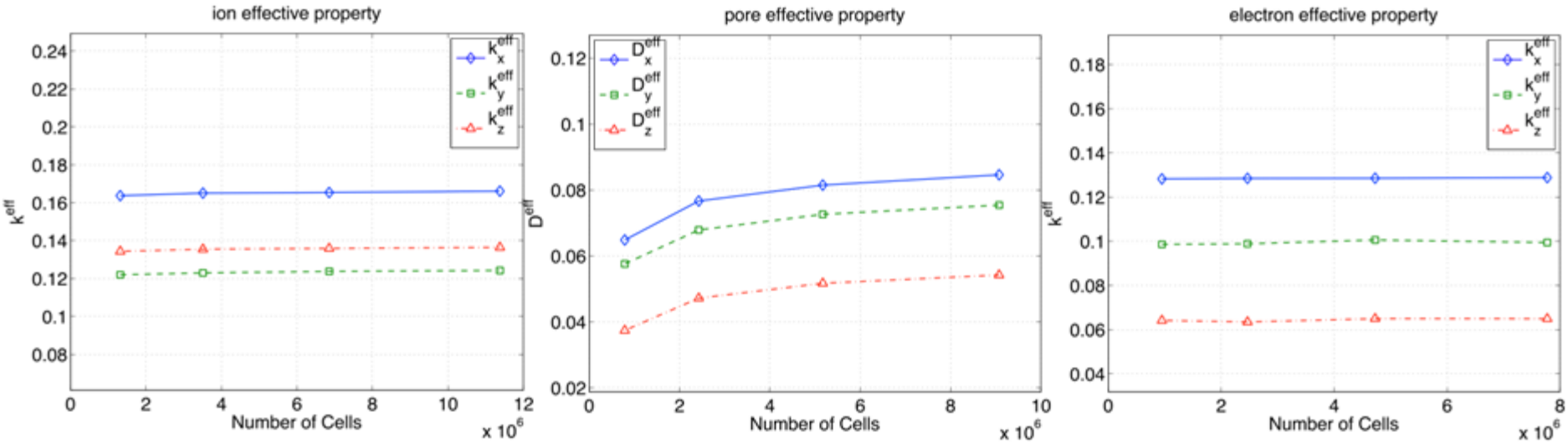

- Both electronic and ionic effective properties converge much faster than Pore phase gas effective properties
- Discrepancies between each directional effective properties due to anisotropic sample structures.
- Electronic effective properties show larger difference between each direction than Ionic values due to larger size of Carbons (d_{carbon}= 25 nm) than Ionomers ($d_{ionomer}$= 10 nm)

Catalyst Sample Polarization

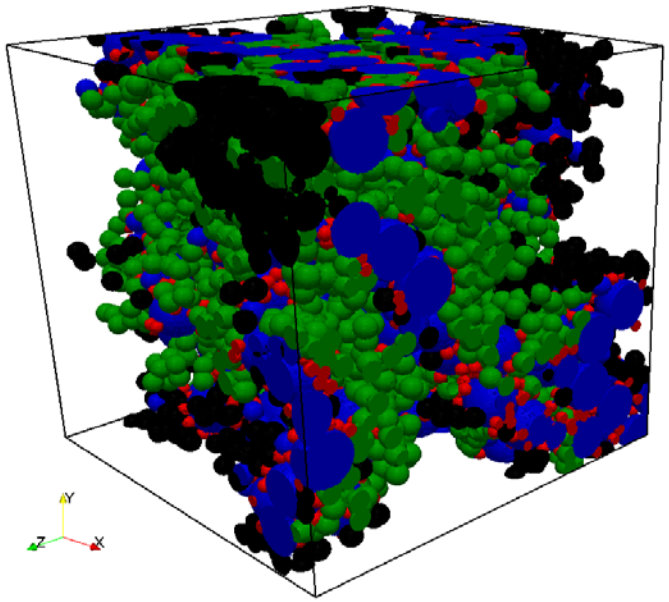

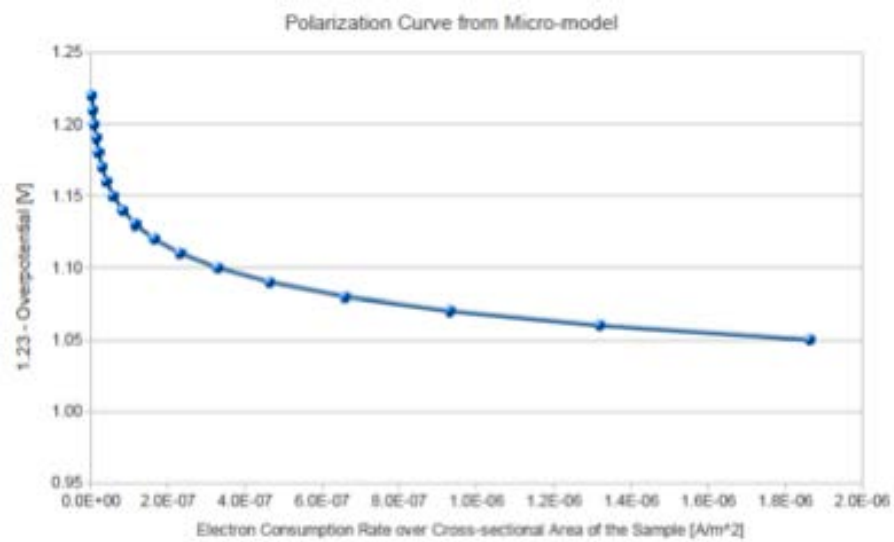

- Polarization Curve is produced for a small sample of catalyst
- Total Catalyst Layer current is a product of the number of samples and the current produced in each

Distribution of Reactants

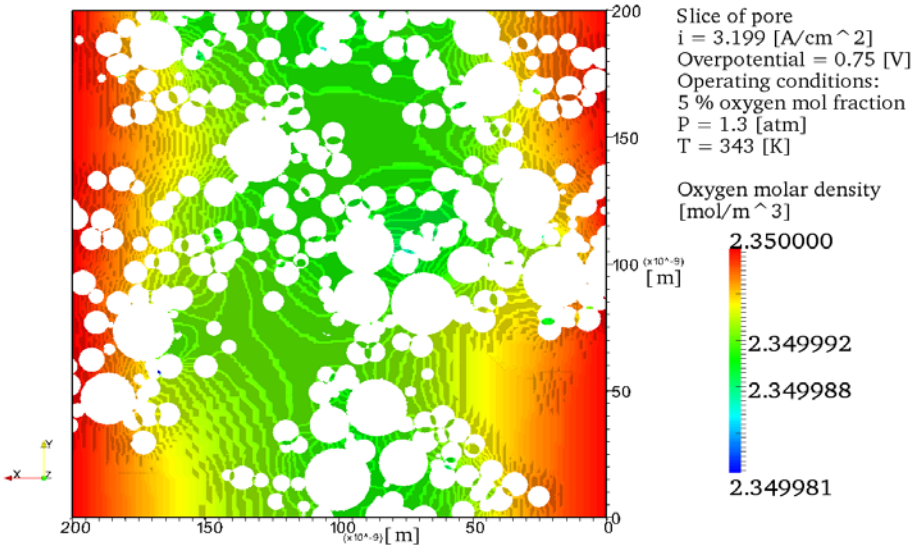

Oxygen in the Pore

- Oxygen is fed on both sides and a minor drop is seen in the center
- The current per unit Pt surface area would appear to be a better benchmark to track
- Currently, unrealistic currents are being used to probe effect of boundary conditions and sampling approach

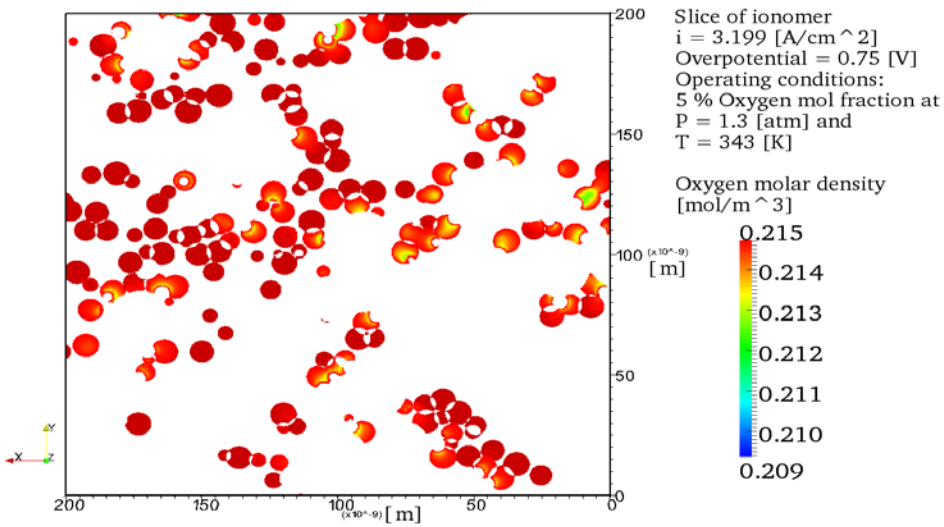

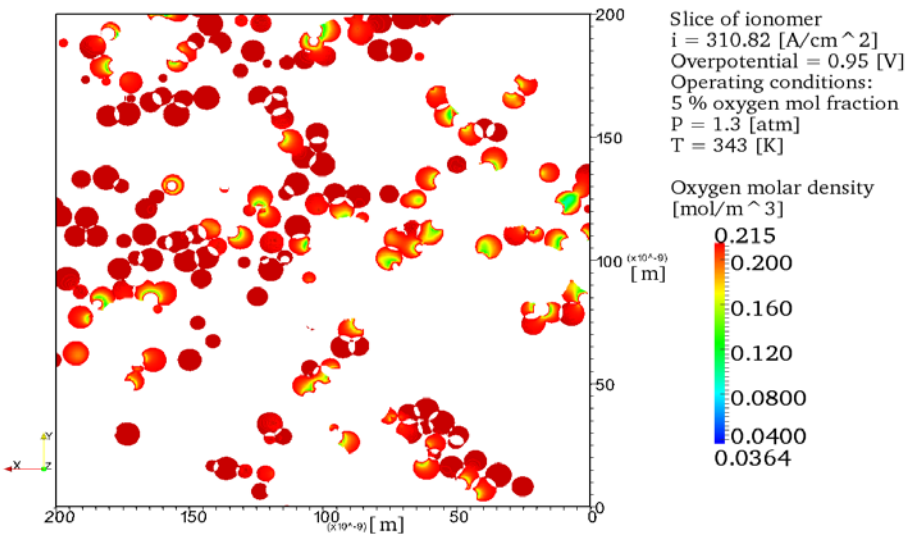

Effective Properties - Electron

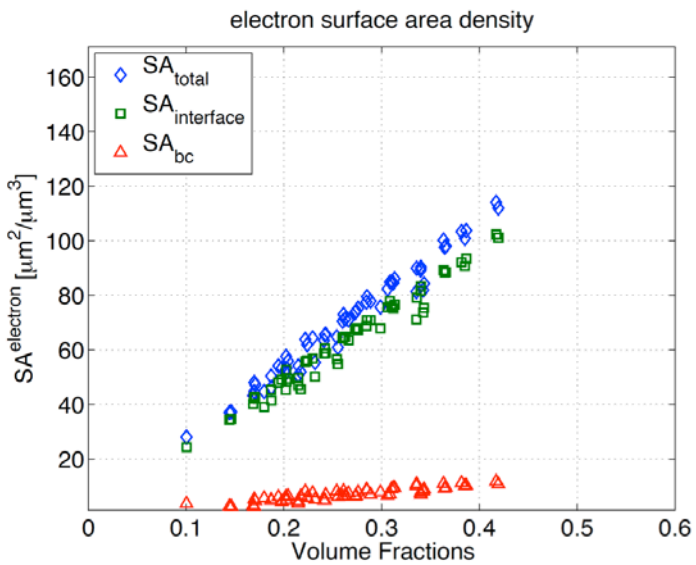

- The surface area of carbon phase changes strongly with volume fraction.
- The tortuosity is very high, but this effect is not usually seen in performance due to higher conductivity assigned to the carbon phase

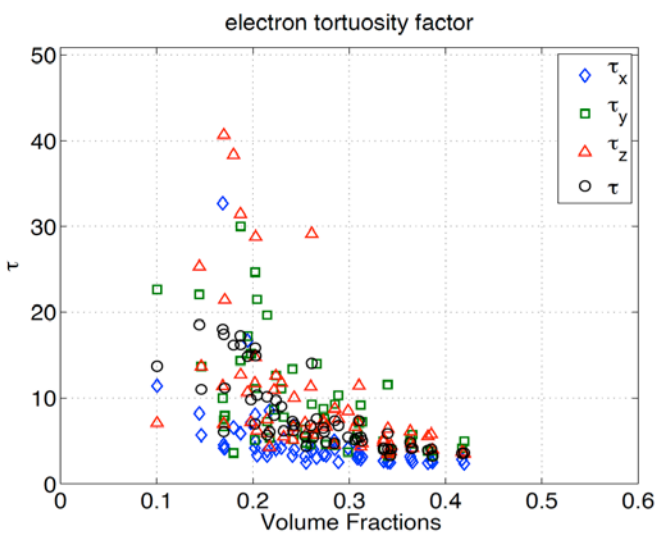

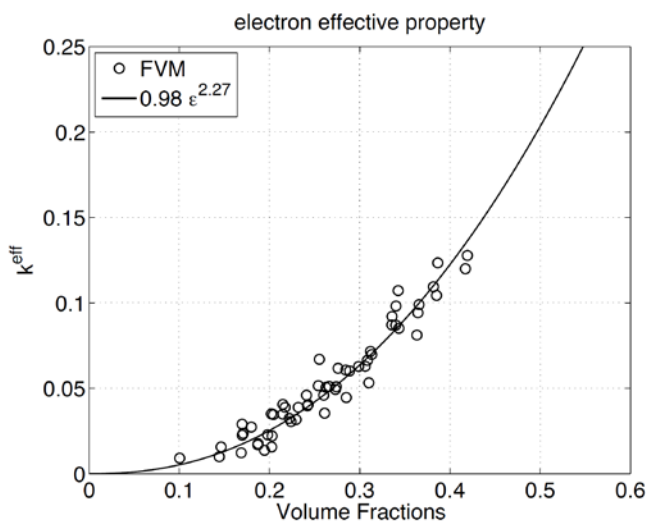

Effective Properties - Pore

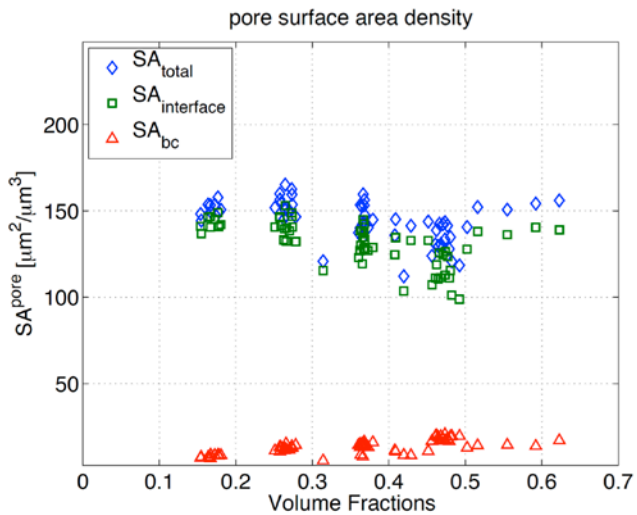

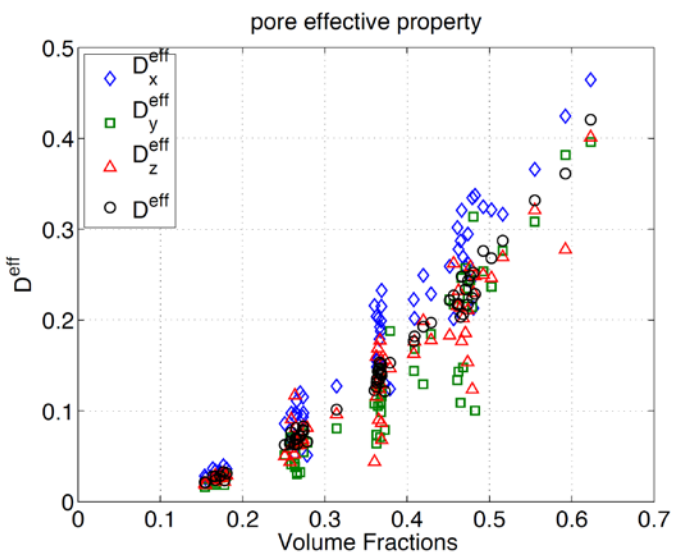

- There is little directional bias in the sample diffusivity based on a non-Knudsen approach.
- A fitted form is developed for comparison with the adjusted form which accounts for Kn effects.

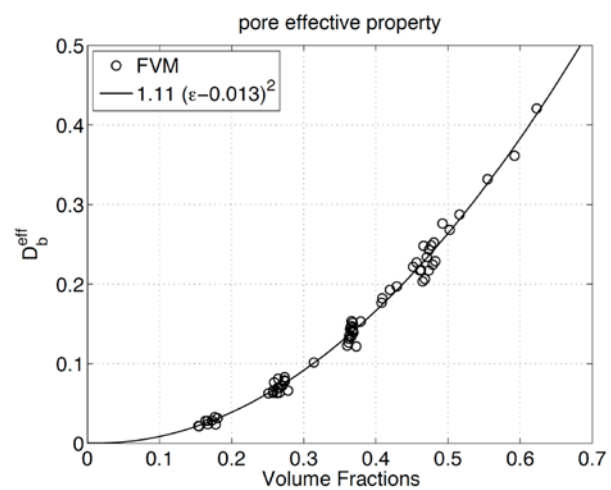

Effective Properties – Pore (Knudsen)

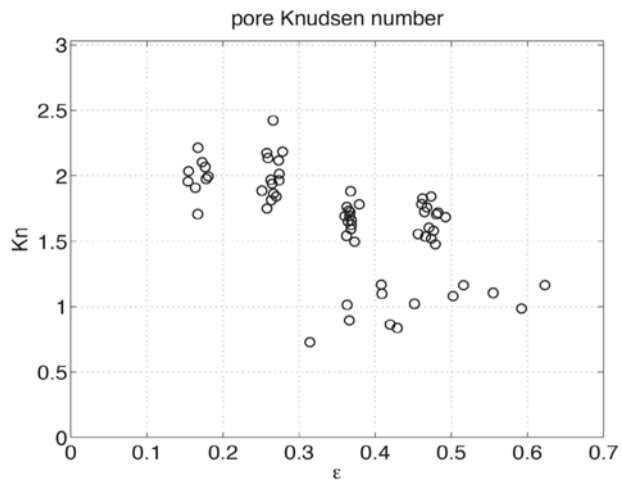

- A Knudsen number is determined based on simulation using a Monte Carlo solver
- As expected, the overall pore diffusivity is reduced, showing a 50% increase in the tortuosity.

$$\mathrm{Kn} = \frac{D_b}{D_{\mathrm{Kn}}} = \frac{\langle \lambda \rangle}{d_{cl}}$$

$$D^{eff}(\mathrm{Kn}) = \frac{\epsilon}{\tau}\left(\frac{1}{D_b} + \frac{1}{D_{\mathrm{Kn}}}\right)^{-1}$$

$$\frac{D^{eff}(\mathrm{Kn})}{D_b} = \frac{\epsilon}{\tau}\frac{1}{1+\mathrm{Kn}} = D^{eff}\frac{1}{1+\mathrm{Kn}}$$

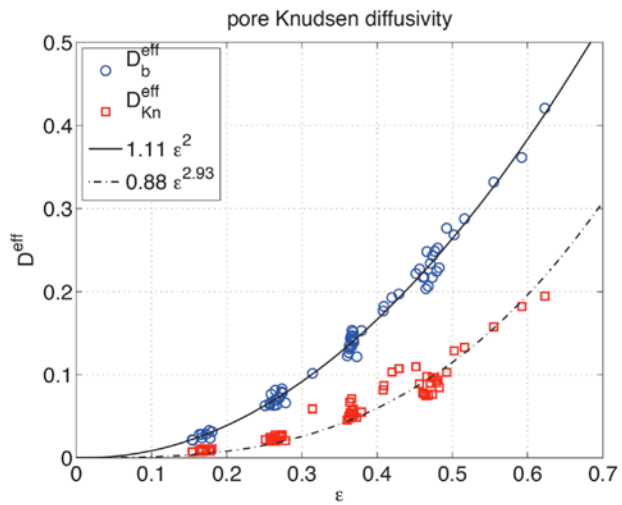

Electrostatic Adsorption: 2wt% TAPHH on Vulcan XC72

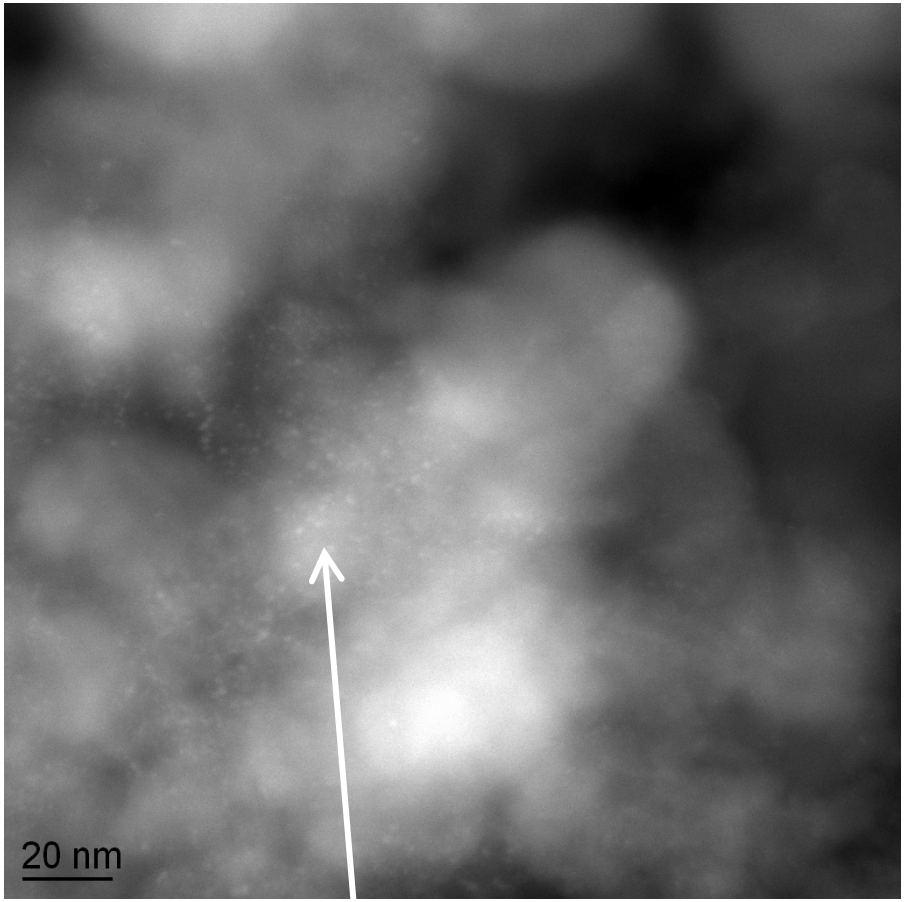

- Similar to CPA on Vulcan
- Most of the Pt preferred to adsorb on the rougher areas of the Vulcan rather than the spheres

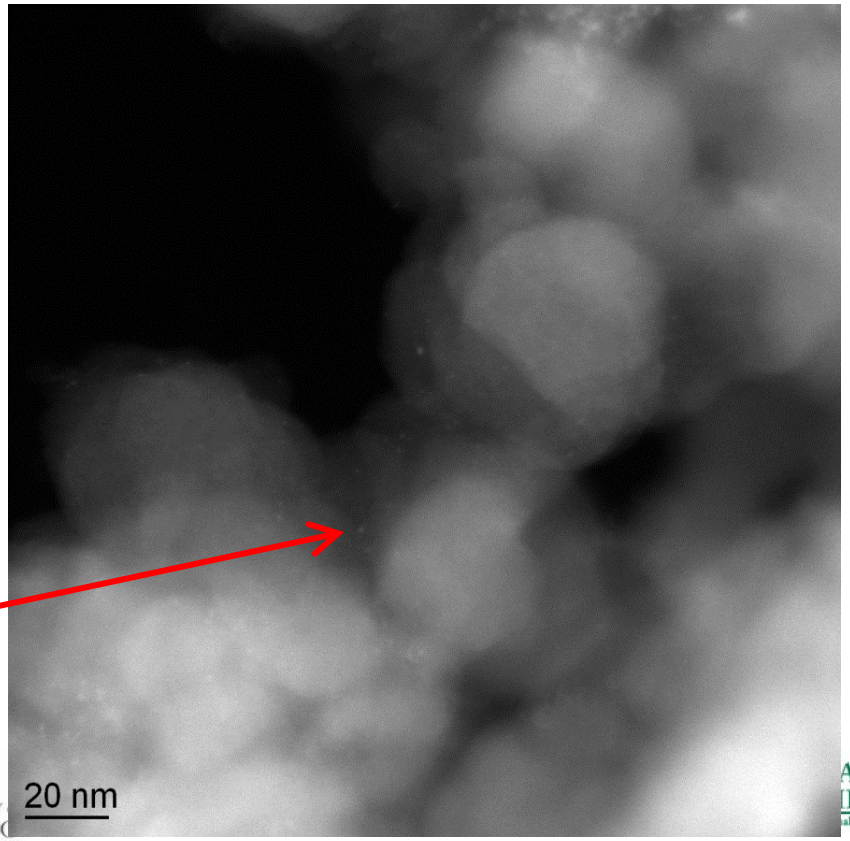

Pt is primarily on the carbon that appears to have more edge sites, rather than the larger spherical particles

Cross-section SEM Pictures and XRD Results at EOT

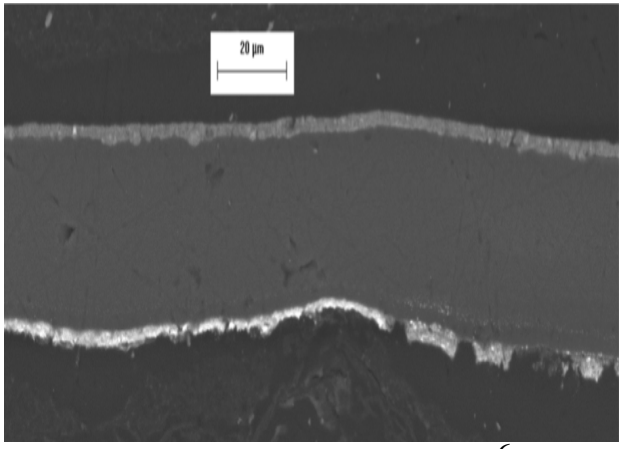

DOE Potential Hold, 2.5 ⌈m, 7.9 nm

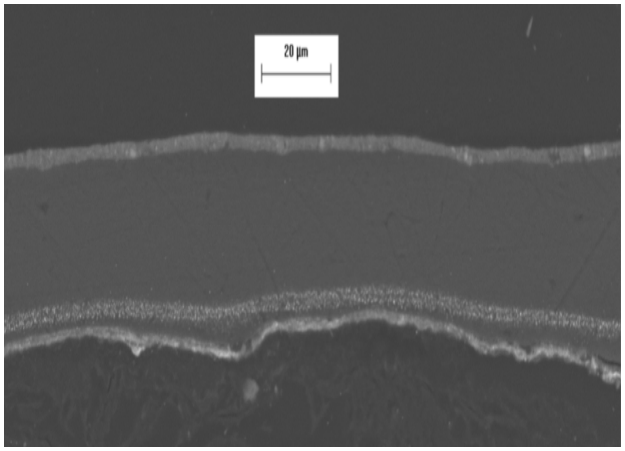

BPS Potential Step, 2.7 ⌈m, 8.3 nm

BOL:
7.7 ⌈m, 2.7 nm

1.2V

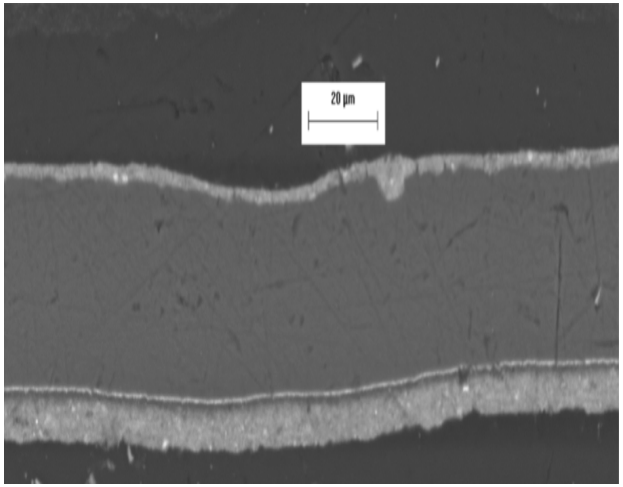

DOE Potential Sweep, 6.4 ⌈m, 6.9 nm

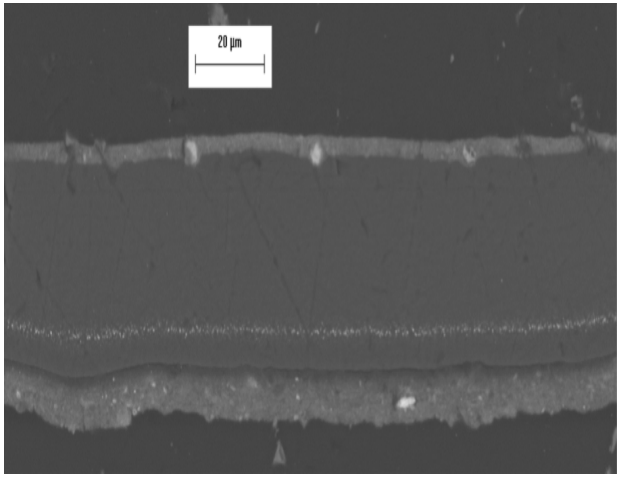

BPS Potential Step, 5.4 ⌈m, 6.7 nm

1.0V

Electrochemical Test of PtY/C

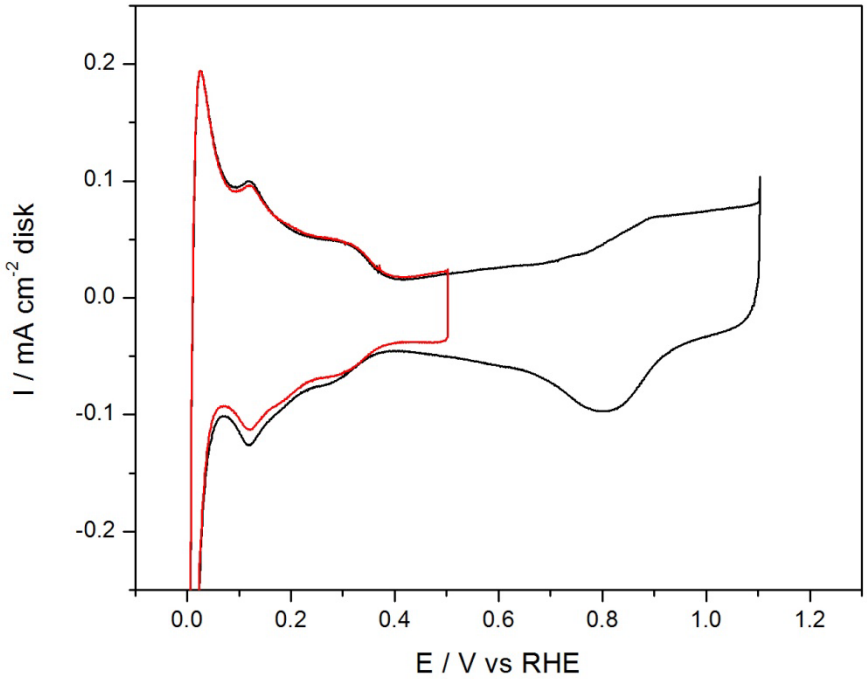

Ar, 0.1 M $HClO_4$, 50 mV/s

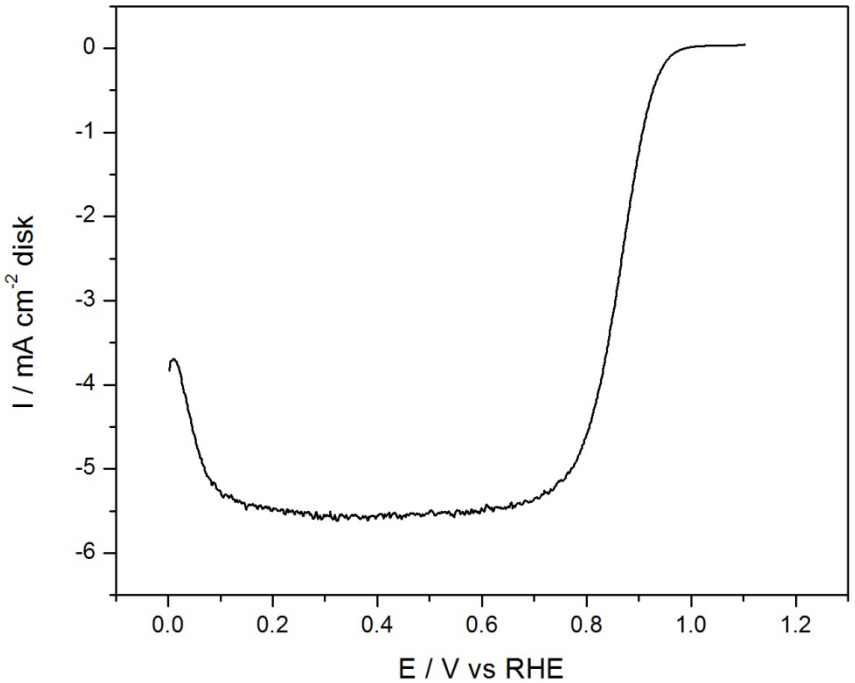

O_2, 0.1 M $HClO_4$, 20 mV/s, 1600 rpm

Results：

SA= 1.2 mA/cm^{2}Pt

Electrochemical Test of PtSc/C

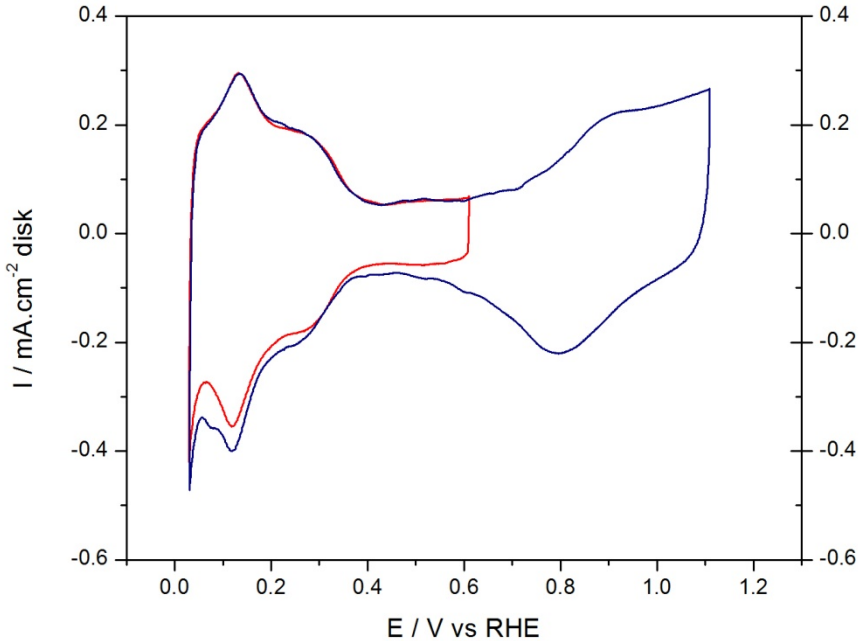

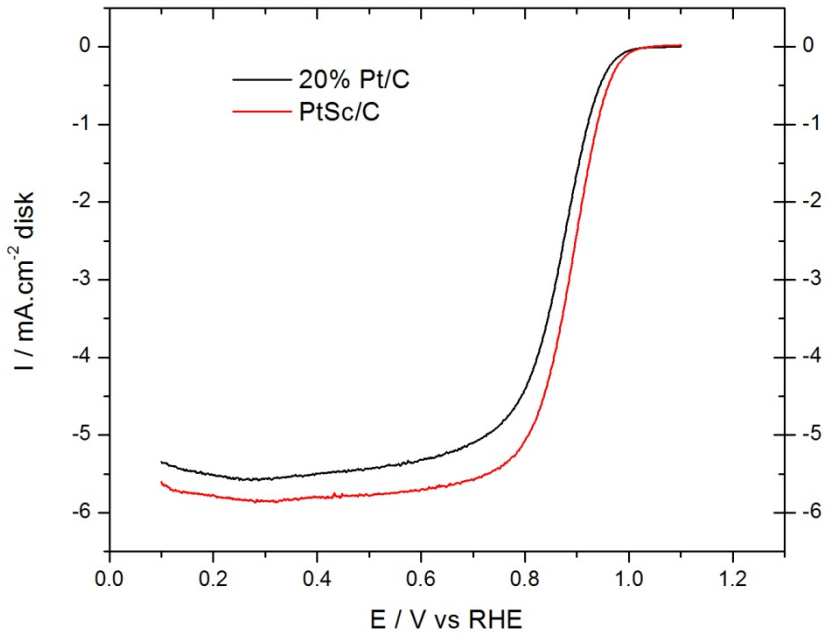

Left: Cyclic voltammograms of PtSc/C in 0.1 M $HClO_4$ at RT. Scanning rate 50 mV/s. Right: ORR polarization curves of 20% Pt/C (from Premetek) and PtSc/C (self synthesized). Scanning rate 20 mV/s.

Results：

SA= 0.94 mA/cm^{2}Pt

Electrochemical Test of PtPd NPLs

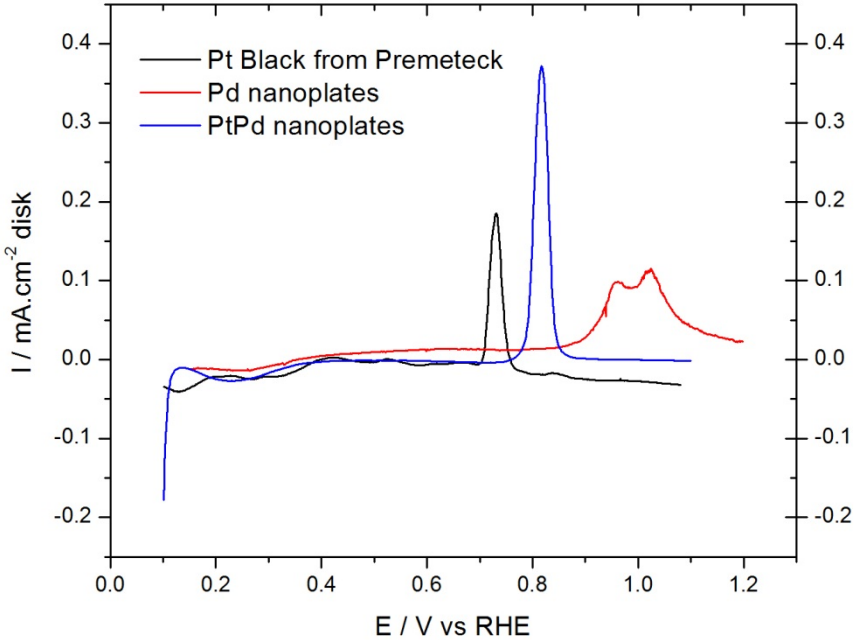

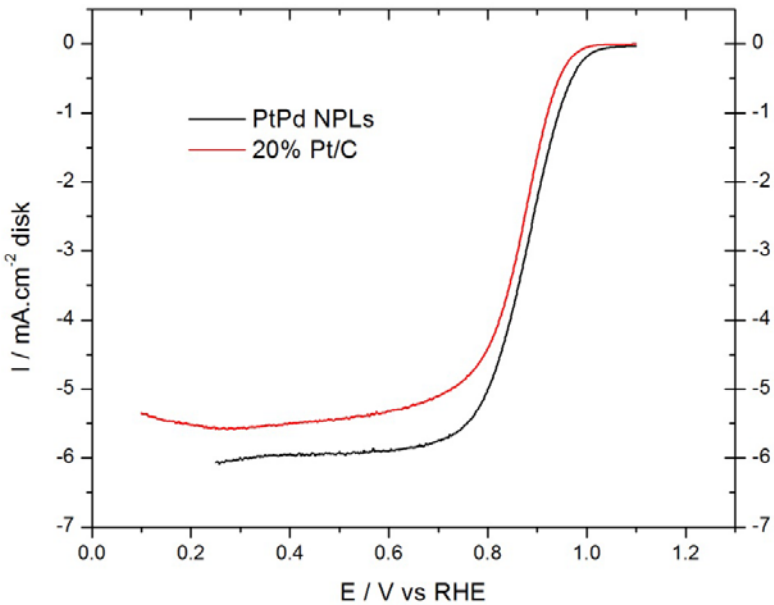

Cyclic Voltammograms (forward scan) for oxidation of saturated CO adsorbed on Pt black (black), pure Pd NPLs (red) and PtPd NPLs (blue) surface in 0.1 M CO free $HClO_4$.
The PtPd CO peak lies in the normal range of Pt surface while CO peak for Pd surface usually lies in a more positive position.

Results：

ESA= 48 m^2/g Pt

SA= 0.48 mA/cm^2Pt

MA= 0.24 mA/µgPt

TEM Result: PtSc nanocrystal

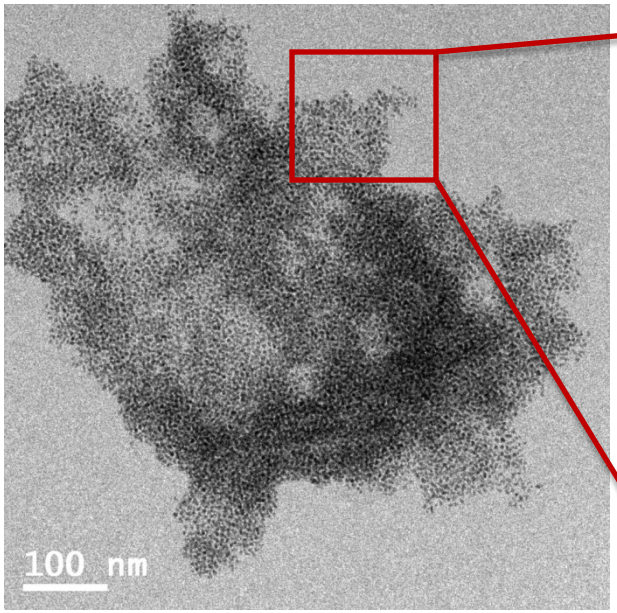

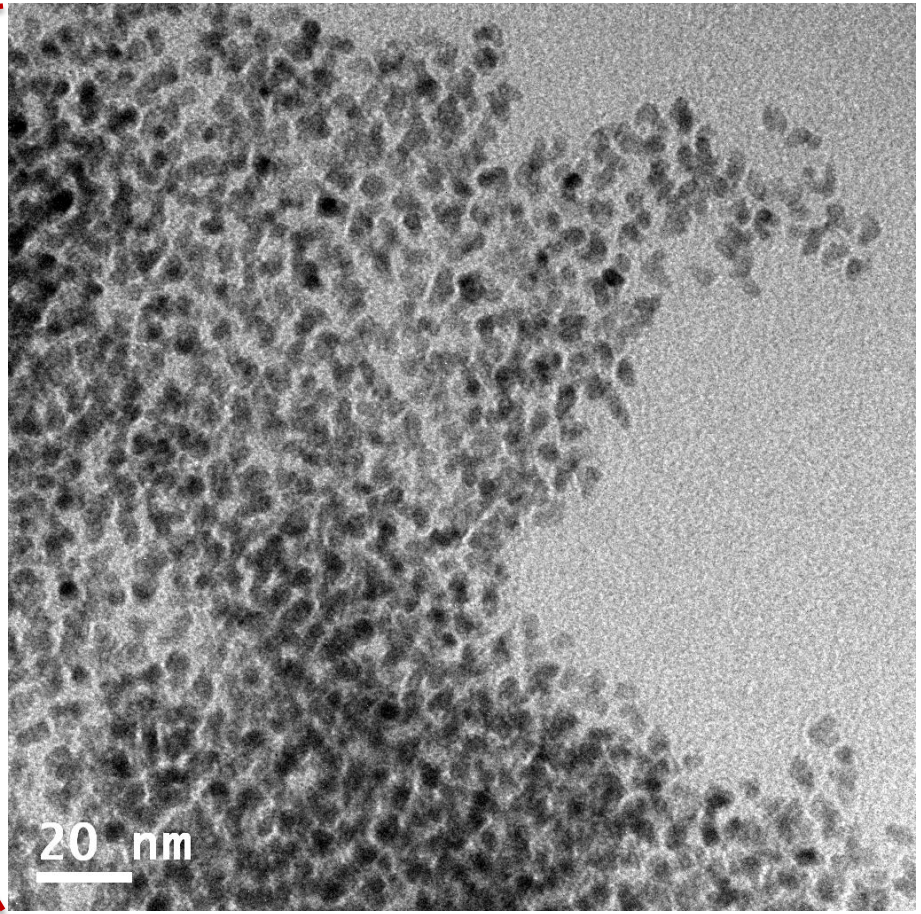

TEM images of as-synthesized PtSc nanoparticles.
Size distribution: 4-7 nm.

Pt Deposition on CePrOx/Carbon

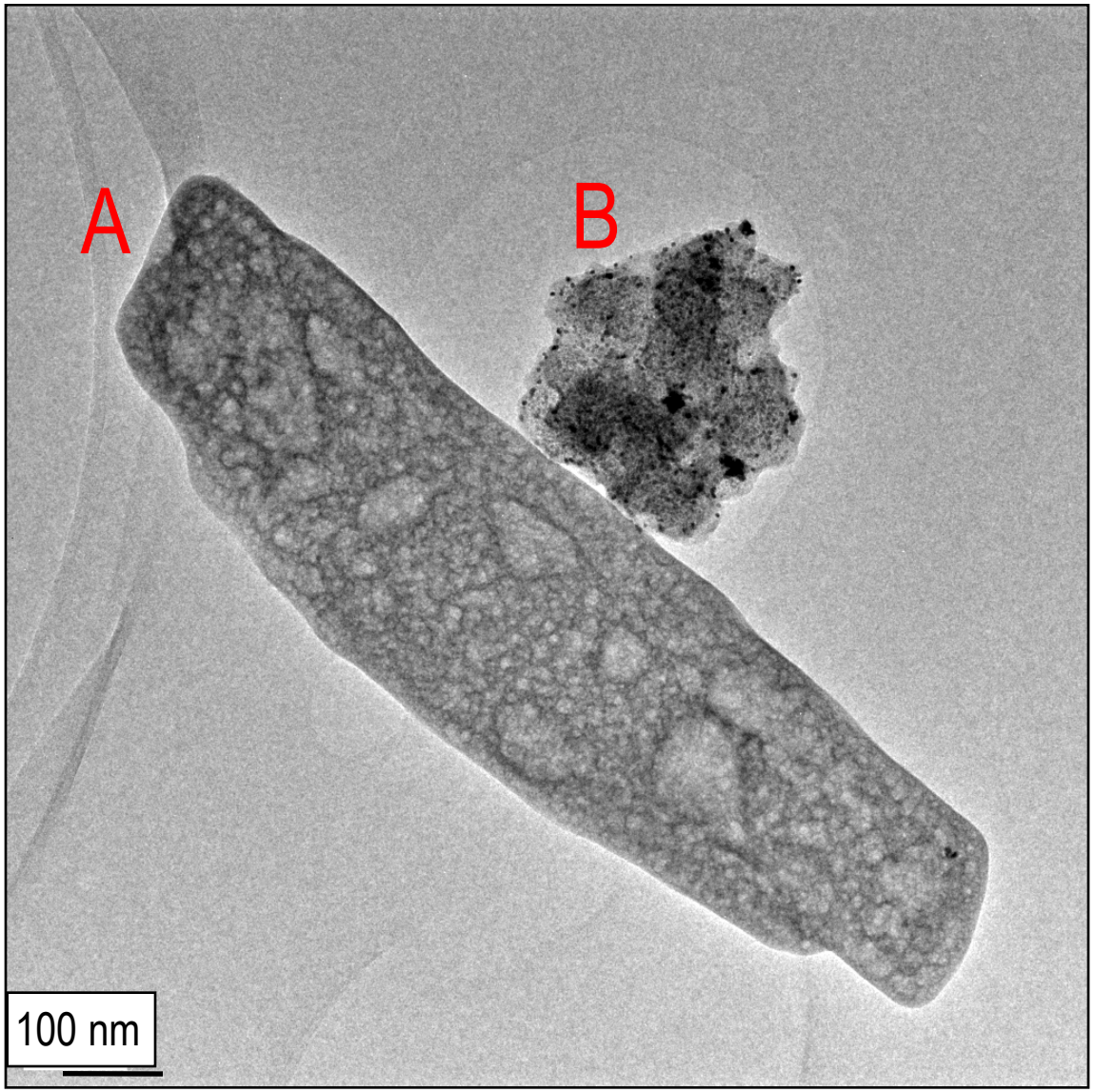

Pt-111117 – 30% Pt on steam activated $(CePr)O_2/C$

Two distinct and separate support-particle morphologies observed:

A: large $(CePr)O_2$ agglomerates with little C or Pt; these agglomerates exhibit significant porosity and are primarily 3 nm $(CePr)O_2$ crystallites

B: aggregated particles rich in C supporting most of the Pt

As with impregnation, Pt still selectively deposits on C.

Pt Deposition on Ce-Pr Oxide

Pt-111207 – 30% Pt on $(CePr)O_2$
(no carbon)

With the absence of carbon, very uniform Pt particle size (~2.5nm), and Pt is well dispersed on surface of oxide.

High and uniform Pt dispersion obtained by removing competition from the carbon

Mediocre RDE results: poor electronic conductivity

Next approach: Mix CePrOx nanopowder to Carbon supported Pt commercial catalyst (TKK)

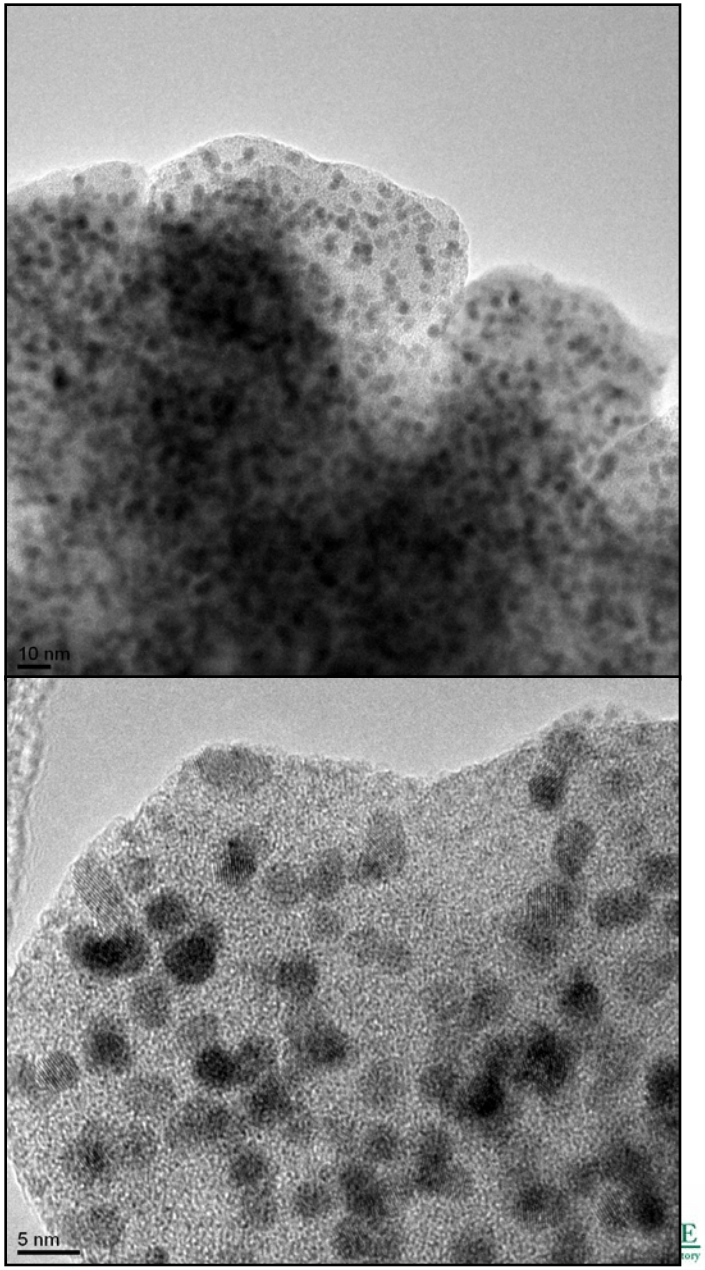

ORR of Catalyst Based on Ceria

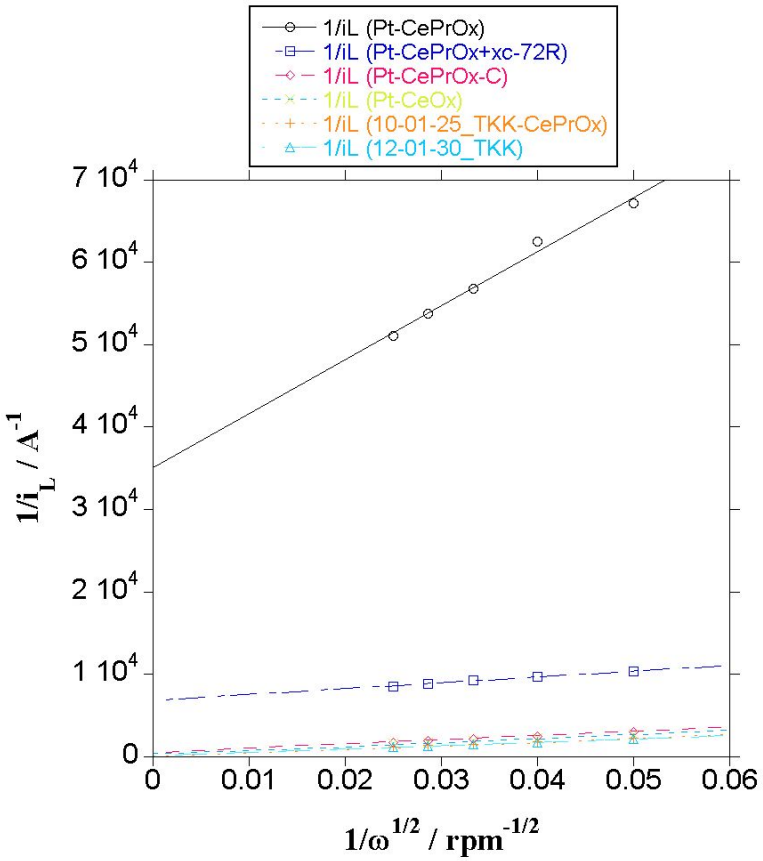

ECSA and %ECSA Loss

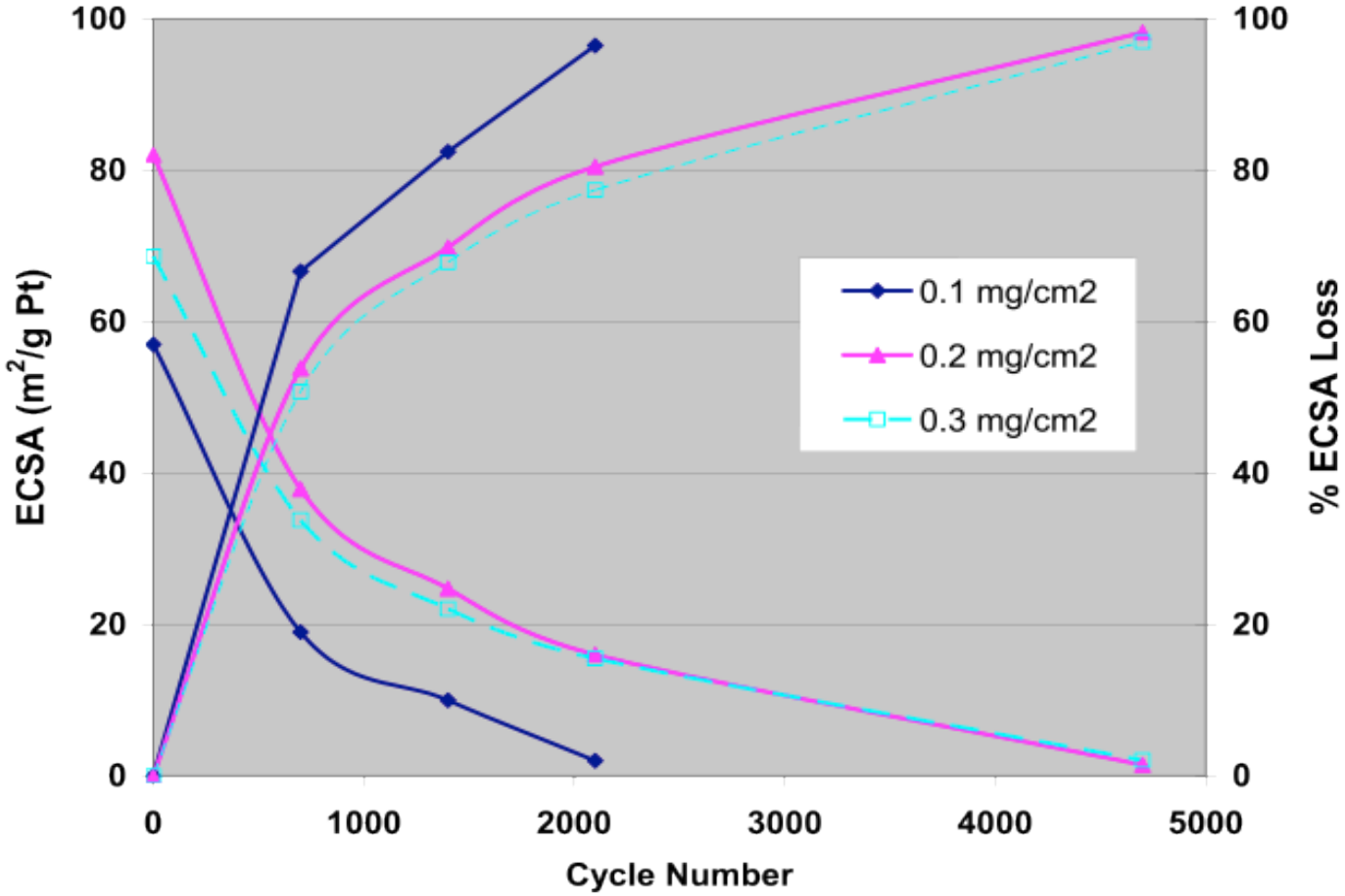

- The MEAs with 0.2 and 0.3 mgPt/cm^2 showed similar %ECSA loss, with lower degradation rate than the MEA with 0.1 mgPt/cm^2.